GROWTH AND CHARACTERIZATION OF BRANCHED GOLD NANOPARTICLES ON SURFACES

A THESIS SUBMITTED TO
THE GRADUATE SCHOOL OF NATURAL AND APPLIED SCIENCES
OF
MIDDLE EAST TECHNICAL UNIVERSITY

BY

NİMET İLKEM EVCİMEN

IN PARTIAL FULFILLMENT OF THE REQUIREMENTS
FOR
THE DEGREE OF MASTER OF SCIENCE
IN
CHEMISTRY

DECEMBER 2014

Approval of the thesis:

GROWTH AND CHARACTERIZATION OF BRANCHED GOLD NANOPARTICLES ON SURFACES

Submitted by **NİMET İLKEM EVCİMEN** in partial fulfillment of the requirements for the degree of **Master of Science in Chemistry Department, Middle East Technical University** by,

Prof. Dr. Gülbin Dural Ünver _____
Dean, Graduate School of **Natural and Applied Sciences**

Prof. Dr. İlker Özkan _____
Head of Department, **Chemistry**

Assoc. Prof. Dr. Emren Nalbant Esentürk _____
Supervisor, **Chemistry Department, METU**

Assoc. Prof. Dr. Hüsnü Emrah Ünalan _____
Co - Supervisor, **Metallurgical and Materials Eng.Dept., METU**

Examining Committee Members:

Prof. Dr. Ceyhan Kayran _____
Chemistry Dept., METU

Assoc. Prof. Dr. Emren Nalbant Esentürk _____
Chemistry Dept., METU

Assoc. Prof. Dr. Hüsnü Emrah Ünalan _____
Metallurgical and Materials Eng. Dept., METU

Assoc. Prof. Dr. Ayşen Yılmaz _____
Chemistry Dept., METU

Assoc. Prof. Dr. Ali Çırpan _____
Chemistry Dept., METU

Date: 25. 12. 2014

I hereby declare that all information in this document has been obtained and presented in accordance with academic rules and ethical conduct. I also declare that, as required by these rules and conduct, I have fully cited and referenced all material and results that are not original to this work.

Name, Last Name: Nimet İlkem EVCİMEN
Signature:

ABSTRACT

GROWTH AND CHARACTERIZATION OF BRANCHED GOLD NANOPARTICLES ON SURFACES

Evcimen, Nimet İlkem
M. S., Department of Chemistry
Supervisor: Assoc. Prof. Dr. Emren Nalbant Esentürk
Co-supervisor: Assoc. Prof. Dr. Hüsnü Emrah Ünalan
December 2014, 82 pages

Branched gold nanoparticles, having sharp edges and tips, provide very high sensitivity to local changes in the dielectric environment, as well as large enhancements of the electric field around the nanoparticles. This makes them very attractive for the applications where special optical properties are needed such as sensing, therapeutic treatments and photovoltaic devices. Nanostructures are needed to be stabilized on some type of support for most of these applications.. This can be achieved either by dispersing synthesized nanoparticles onto the surfaces or by directly synthesizing them on the surface. Second approach can be more practical as it is eliminating the extra step of nanoparticle dispersion by methods such as spin coating or drop casting.

In this study, branched Au nanoparticles were synthesized on surfaces of three different supports (glass, ITO, Si-wafer). Parametric study was performed to investigate the effect of reactant concentrations, seed type and pH of the growth media on the quality of products. Optimum conditions were determined for synthesizing nanostructures in high yield and structural purity. Characterization of

nanostructures was done by detailed analysis via scanning electron microscope (SEM), energy dispersive X-Ray (EDX) and X-Ray Diffraction (XRD) methods. The analyses showed that all of the nanostructures synthesized at optimum conditions have branched morphologies with sizes of ca. 450 nm and they are well dispersed on the support surface.

Keywords: Nanoparticles, anisotropy, branched gold nanoparticles, growth, surface, substrates, seed-mediated growth, Si-wafer

ÖZ

DALLANMIŞ ALTIN NANOPARÇACIKLARIN YÜZEY ÜZERİNDE BÜYÜTÜLMESİ VE KARAKTERİZASYONU

Evcimen, Nimet İlkem
Yüksek Lisans, Kimya Bölümü
Tez Yöneticisi: Doç. Dr. Emren Nalbant Esentürk
Ortak Tez Yöneticisi: Doç. Dr. Hüsnü Emrah Ünalan
Aralık 2014, 82 sayfa

Tüm nanoparçacıklar içinde, sivri kenarlara ve uçlara sahip olan dallanmış altın nanoparçacıklar, nanoparçacık etrafındaki elektromanyetik alanda büyük gelişmelerin yanı sıra yalıtkan ortamlardaki küçük değişikliklere karşı da yüksek duyarlılık sağlamaktadır. Bu durum altın nanoparçacıkları özel optik özellikler isteyen iyileştirici tedavilerde, biyoalgı ve güneş hücresi uygulamaları gibi alanlarda kullanımını oldukça ilgi çekici yapmaktadır. Bu uygulamaların bir çoğu için nanoparçacıkların bir destek üzerinde sabitlenmesi gerekmektedir. Bu sabitlenme durumu sentezlenmiş nanoparçacıkların yüzey üzerine dağıtılması ya da nanoparçacıkların doğrudan yüzey üzerinde sentezlenmesi yoluyla gerçekleştirilebilir. Nanoparçacıkların döngü kaplama ya da damla döküm gibi yöntemler yoluyla yüzey üzerinde dağıtılmasından kaynaklanan fazla adımları elediğinden, ikinci yöntem daha pratik olabilir.

Bu çalışmada dalllanmış altın nanoparçacıklar üç farklı desteğin (cam, ITO ve silicon levha). yüzeyi üzerinde sentezlenmiştir Tepkimelerde yer alan kimyasalların derişimleri, çekirdek tipi ve büyüme ortam pH'ının ürünlerin kalitesine olan etkisini incelemek amacıyla parametrik çalışma yapılmıştır. Yüksek verim ve yapısal saflıktaki nanoyapıları sentezlemeye en elverişli koşullar belirlenmiştir. Nanoyapıların karakterizasyonu taramalı electron mikroskobu (SEM), enerji dağıtıcı X-ray spektroskopisi (EDX) ve X-ray kırınımı (XRD) yöntemleri ile yapılmıştır. Analizler, uygun koşullarda sentezlenen nanoyapıların yaklaşık 450 nm boyutunda dallanmış bir yapıya sahip olduklarını ve yüzey üzerindeki dağılımlarının iyi göstermektedir.

Anahtar Kelimeler: Nanoparçacık, şekilleri küreselden farklı, dallanmış altın nanoparçacık, büyüme, yüzey, substrat, tohum aracılı büyüme, silikon levha

Don’t let him forget that;

“Science also serves humanity.”

To the precious men of my life:

My father, my brother and my moustache groom Erhan

ACKNOWLEDGEMENTS

I would like to express my gratitude to my supervisor Assoc. Prof. Dr. Emren NALBANT ESENTÜRK, for her guidance, support, encouragement, teaching me how to become an ethical scientist and helping me in not only my thesis but also in my life.

I would like to thank to my co-advisor Assoc. Prof. Dr. Hüsnü Emrah ÜNALAN for his valuable help and kind attitude.

I owe my gratitude to Şahin COŞKUN for his valuable comments, contribution to this work, remarkable effort for booking SEM session and for our conversation which makes our SEM session enjoyable.

I would like to thank to my lab-mates; Doruk, since he made me to realize NanoClusMate; Çağla, for sharing her knowledge about the research; Asude, for answering my all questions without complaining; Esra for solving my practical problems with a small touch; Cansu, for her remarkable effort to put a smile on my face; Çiğdem and Serra for their help during my studies and to all of them for make me feel like I was here for a long time and make B-37 more than classical laboratory.

There is no word to define my thankfulness to Ayda and Merve. They never let me give up and make me believe in myself regardless of the distance.

I am deeply grateful to Gizem and Melike. No matter where they are, they always listen to me, give me the feel of having hug and always try to produce a solution to my problems.

I would like to thank Anıl, Edalinka, Seval, Zerrin, Eda, Cihan, Sedef, Mühdan, Seher, Çiğdem, Duygu, Göktuğ, Didar, Sertaç, Serkan, Cahide for their true friendship and always being there for me.

A special thanks goes to my roommates, Ceren, Ziya and my brother-like friend Özgür for listening me any times I need, for the coffee and tea with knock on the door, meal sessions having together, and tolerating me over the years. They were the ones who make Ankara my homeland, my home.

I would like to express my sincere gratitude to Erdem TÜRKŞEN for being my first mentor about the life; Selen AVCI for being the woman who knows what I thought without using words and my mother Nuran EVCİMEN just for her existence. Even if they passed away from this world so early, I know that they will be with me forever.

I would also like to thank my father Bülent EVCİMEN for giving me the sense of resistance; my aunt Saime ŞEN because she never let me feel lack of my mother; my brother Taylan Ulaş EVCİMEN for his support, guidance and insistence about providing me a better life.

The last but not the least, I would like to express my thankfulness to Erhan TÜRKMEN for his ownership of this thesis, patience, encouragement, support and endless love. Without him, it was not possible to complete this study and one part of my soul would be missing.

TABLE OF CONTENTS

LIST OF FIGURES

FIGURES

LIST OF TABLES

TABLE

LIST OF ABBREVIATIONS

1 D	One dimensional
2 D	Two dimensional
3 D	Three dimensional
^{o}C	degrees Celsius
APTMS	3-aminopropyl-trimethoxysilane
ca.	Circa (prediction in amount)
CTAB	Cetyltrimethylammoniumbromide
EDX	Energy Dispersive X-ray Spectroscopy
EGFR	Epidermal Growth Factor Receptor
et al	et alii (and others)
g	gram
IR	Infrared Spectroscopy
ITO	Indium Tin Oxide
i.e	id est (in essence)
LED	Light Emitting Diode
LSPR	Localized Surface Plasmon Resonance
m^2	square meters
mm	millimeter
mg	milligram
mL	milliliter
mmol	millimole
MO	molecular orbital
MPTMS	3-mercaptopropl-trimethoxysilane
NIR	Near Infrared
nm	nanometer
PVP	Polyvinyl pyrrolidone

SERS	Surface Enhanced Raman Scattering
Si	Silicon
SPR	Surface Plasmon Resonance
UV-Vis	Ultraviolet-Visible
XRD	X-Ray Diffraction

CHAPTER 1

INTRODUCTION

1.1. Motivation for the Study

Nanoparticles have properties between individual atoms and bulk materials. It has been observed that materials have unique properties (i.e. chemical, optical, mechanical and electrical) when their sizes are reduced to nano scale. These size and in most cases shape dependent characteristic of nanomaterials make possible tuning and controlling materials' properties to fit them particular applications. Therefore, nanomaterials have become very active research avenue for last couple of decades.

Among all nanoparticles the ones made of Au with anisotropic morphologies have attracted great deal of attention because of their special optical and plasmonic properties. In particular, the ones with branched morphologies absorb the light strongly in the near IR region and produce strong electric field strength at their tips.[1–4] Therefore, these structures are great candidates to be used in photonics, electronics as well as sensing, imaging and biomedical applications.[4–8]

Various synthesis methods have been developed to fabricate Au nanoparticles with anisotropic structures.[9–11] Solution phase methods where chemical reduction of Au salt in the presence of surface directing agent (i.e cetyldimethylammoniumbromide (CTAB) and poly-vinylpyrrolidine (PVP)) takes place have been frequently preferred. The use of one of these methods called "seed-mediated growth method" has yielded the synthesis of Au nanoparticles with different sizes and shapes.[12] The method embody many advantages such as taking place in aqueous media, being

relatively simple, possibility of controlling properties of nanoparticles (size and morphology) by simple adjustments in reaction parameters (i.e concentration of reactant, pH of the growth media).[13]

Many applications in nanotechnology require nanomaterials to be stabilized on surfaces. Two different approach can be followed to achieve this: i) transferring nanoparticles synthesized in solution phase to the substrate surface by techniques such as spin coating or drop casting, or ii) growing nanoparticles directly on surfaces. The second approach is very practical if the targeted nanostructures can be synthesized on the surface of application. Up to date, spherical and rod shaped Au nanoparticle have been synthesized on three different surfaces (i.e. Si-wafer, mica, ITO) by using seed mediated approach.[14,15] On the other hand, to our knowledge, surface synthesis of branched Au nanoparticles which have superior optical properties compared to rods and spheres, have not been reported yet.

In this study, branched Au nanoparticles were synthesized on Si-wafer, ITO and glass surfaces. The seed mediated synthesis method was used to grow the desired nanostructures. The important parameters of the procedure such as concentrations of reactants, pH of the growth media and seed characteristics were modified to synthesize the nanostructures in high yield and morphological purity. Having nanostructures with enhanced optical properties on surfaces which are suitable for further device uses make the prepared system very promising for solar cell and sensing applications.

1.2. Nanoparticles

In Greek Language *"nano"* prefix means dwarf or extremely small. In proper way to etymological origin of *"nano"*, nanoparticle defined as an aggregate of atoms bonded together with a radius between 1 and 100 nm which consists of typically 10-10^5 atoms.[16] (Figure 1.1)

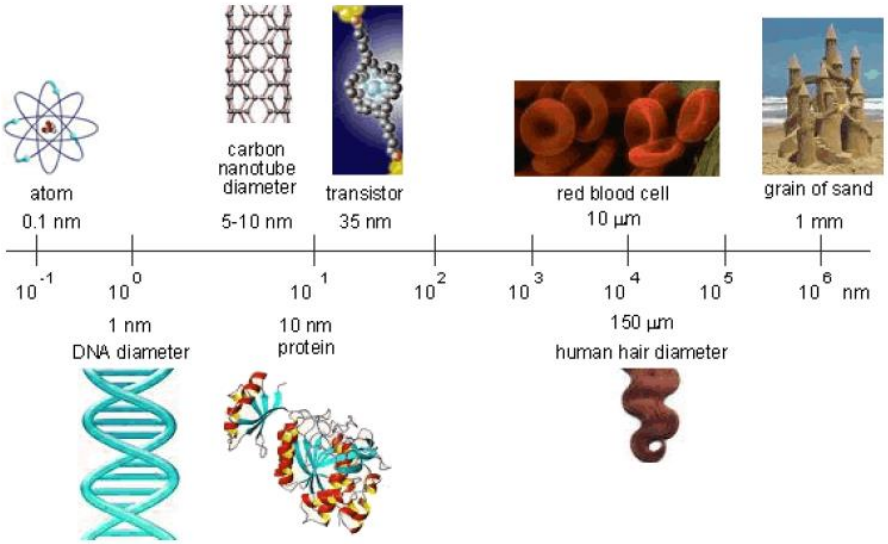

Figure 1.1. Nanoscale of life.[125]

The use of particles in nano size goes back to ancient times. For example, the controlled supplements of ceramic matrix was being provided by natural asbestos nanofibers 4500 years ago.[17] Moreover, due to their intriguing color, metal nanoparticles have been used as colorant in ceramics and paintings for more than

2000 years.[18] For instance, Lycurgus Cup produced by Romans in fourth century appears green in day light but becomes red when illuminated from inside.[19] (Figure 1.2.B) The presence of trace quantities of Au nanoparticles is responsible for this complex color. Today, nanoparticles can find various applications in different fields. For instance, silica particles can be used as anti-caking agent[20] in food industry and titanium or zinc oxide particles can be used in cosmetic (i.e. sun screens).[21]

Figure 1.2. The picture of (A) Faraday's gold colloids (B) Lycurgus Cup (green with reflected light, red when illuminated from behind.[126,127]

In the mid-nineteenth century, Michael Faraday attributed the red color of colloidal Au to its finely divided state[22] (Figure 1.2.A) and his early speculative experiments laid the foundation for some of the current optical and biological applications of Au nanoparticles. About a century later, Richard Feynman set the stage for the nanotechnology revolution in his famous lecture "there is plenty of room at the bottom", in which he predicted the inevitable miniaturization of devices into nanometer size with enhanced performances.[23] With the advent of new analysis

techniques as well as the availability of innovative synthesis methods, new nanoparticles have been developed with better understanding during last decades. The unusual physicochemical and optoelectronic properties depend on both individual and collective properties of nanoparticles and their sizes and shapes. This provides tunable materials with broad potential applications, and production of structurally complex nanoparticles with further enhances in their functionality.

Among all nanosized materials, metal nanoparticles have attracted great deal of attention for centuries as the examples given above. Metals, like most other materials, show unique characteristics when their size is reduced to nanoscale from bulk size.[16] Having high surface to volume ratio is one of the distinctive characteristics of these materials in nanoregime. For instance, the surface area of a gram of TiO_2 particles increases from 1.41 m^2/g to 281.69 m^2/g when the size decreases from 100 μm to 5 nm. Thus, high surface area along with high surface activity of nanomaterials makes them great candidates for applications such as antibacterial agents, sensors and catalysts.[24] Large surface to volume ratio of nanoparticles give rise to larger proportions of constituent atoms at the surface of nanomaterials.[25] By the way, they present ideal systems to study surface effects on the conduction electrons.[26]

Physicochemical properties of nanoparticles such as electrical, optical and magnetic are size and shape dependent. These special properties are resulted from quantum confinement effect. Quantum confinement effect arises when the location of a particle is trapped to a very small region of space. Likewise, it is observed when the size of nanoparticle is too small to be comparable to the wavelength of electron.[27]

The band gap is the nanoscale related electric property of a material and it increases with the decreasing size of material. (Figure 1.3) Band gap is defined as an energy range where no electron states can exist and it defines the conductivity characteristic of materials. Band gap of a material increases with decreasing size of a material. As

a result, a metallic material can change from being conductive to being semiconductive, while a semiconductor can become insulating when its size comes into nano range.[24]

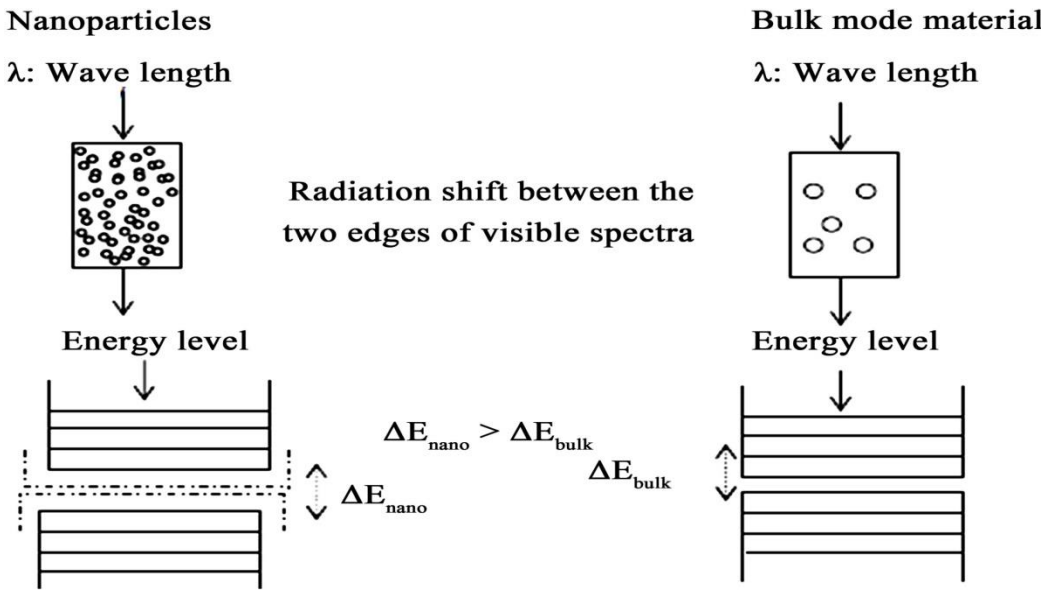

Figure 1.3. Quantum confinement effect on bandgap.[128]

For example at low temperature, for bismuth nanowires electrical resistance increases with wire diameter.[28] In addition, silicon single-crystal nanowires can be counted as insulator.[29]

When the size of particles decreases to nanorange from bulk size, some interesting optical properties arises. For instance, 5 nm Au nanoparticles absorb light at 520 nm. On the contrary, bulk Au is reflective at this wavelength. Moreover, while color

of Au nanosphere is red, color of bulk Au is yellow.[24] Color is resulted from the collective oscillation of the electrons in the conduction band, known as the surface plasmon excitation. In addition, optical property is related to interaction of electromagnetic radiation with matter. When the wavelength of light is much larger than nanoparticle size it can set up standing resonance conditions. Light in resonance with the surface plasmon oscillation causes the free electrons in the metal to oscillate. By the coherent motion of the conduction band electrons from one surface of the particle to the other upon interaction with an electromagnetic field, surface plasmon resonance (SPR) is created.[30] The oscillating charges can also be confined and enhanced on the surface of nanoparticle, in which case it is called localized surface plasmon resonance (LSPR).[31] The optical properties of noble metal nanoparticles in UV-vis-NIR spectral range are mainly determined by LSPR.[12] The oscillation frequency is usually in the visible region for Au giving rise to strong surface plasmon resonance absorption. When metal nanoparticles are enlarged, their optical properties change slightly. On the other hand for semiconductor nanoparticles even simple change can alter the optical properties of nanoparticles.[30] (Figure 1.4)

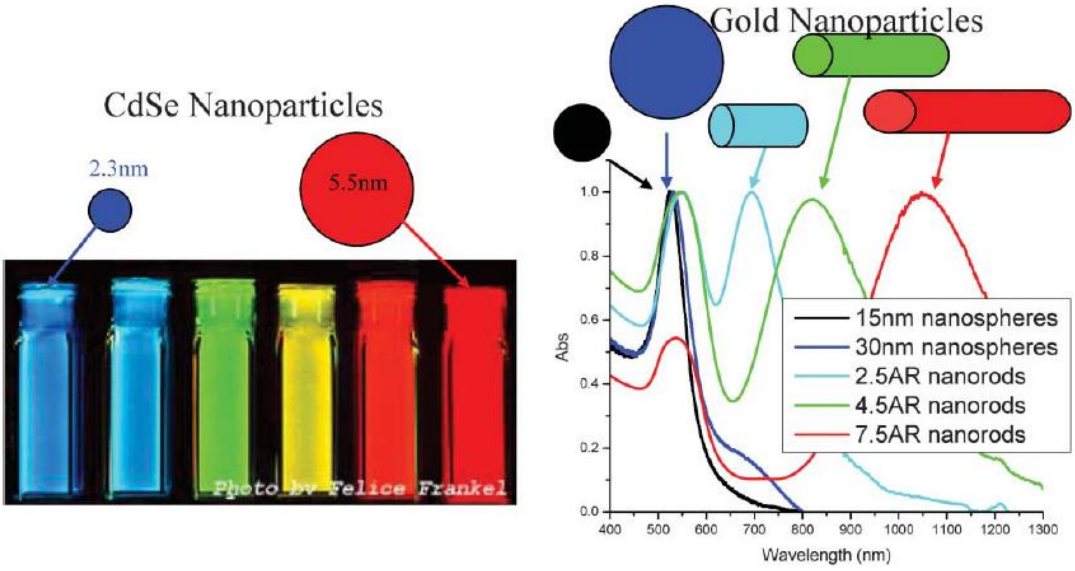

Figure 1.4. Fluorescence nanoparticles of semiconductor (CdSe) nanoparticles (left) Absorption of gold nanoparticles (right).[30]

The magnetic properties of nanomaterials arise mainly from the orbital motion of their electrons.[32] Below a certain diameter, which depends on the material, a particle is single domain. In single domain nanoparticle, all spins are aligned in the same direction and the particle is uniformly magnetized. As a result, some nanoparticles lie iron, nickel show response to an applied magnetic field.[33]

Electromagnetic field of nanoparticles is resulted from the synergetic work of their electric field and magnetic field. The interaction of the incoming laser radiation with electrons on metal surface, which activates surface plasmons or collective oscillations of the metal electrons, causes the enhancement of field.[34] Enhanced electromagnetic field on nanoparticles' surface forms the origin of surface enhanced raman scattering (SERS) effect.[35] Electric field lines concentrated on highly curved surface, which is called as "lightning rod effect".[36] It means that anisotropic metallic

nanoparticles are great candidates for SERS substrates with respect to isotropic ones. [1]

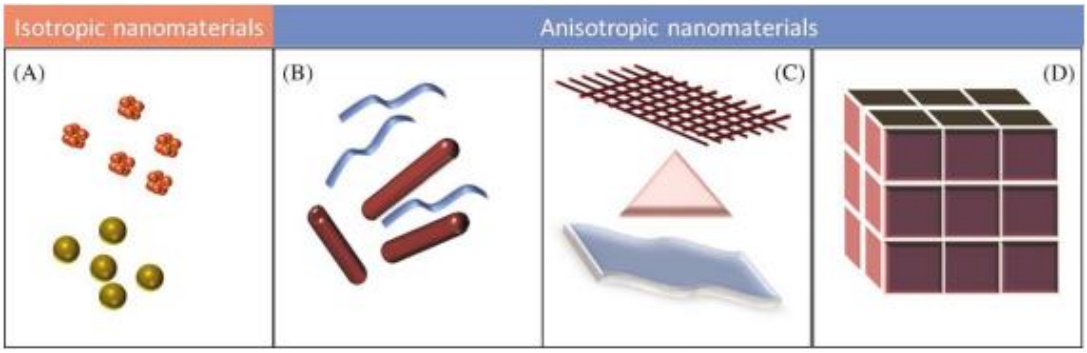

Figure 1.5. Isotropic and anisotropic nanoparticles.[25]

Particle anisotropy can lead to nanoparticle properties which are difficult to obtain in spherical isotropic particles. Degree of anisotropy of a particle can be increased by combining lower dimensional nanostructure with same or higher dimensional nanosystems.[37] Many examples can be given to anisotropic nanoparticles (Figure 1.5) in the literature like nanorods[38–43], nanowires[38,39,44,45], nanotubes[46] as 1D; triangles[47,48], sheet[49,50] as 2D; pyramids[51,52], stars[9,53,54], flowers[55], as 3D nanomaterials. Anisotropic nanoparticles can be used for targeting cancer cells for example in photo thermal studies.[56,57] Since they are biocompatible, easy to conjugate biologically and have strong SPR, these nanoparticles can be used as an effective contrast agent in NIR imaging application [58]. They can be used for making surfaces hydrophobic.[59] Anisotropic nanomaterials can be useful for sensing by taking the advantage of their SPR exhibition.[60]

Among all metal nanoparticles, Au nanoparticles have attracted great deal of attention. Their special characteristics, application areas and detailed synthesis methods will be given in following sections.

1.3. Gold Nanoparticles

Gold is one of the first metals known by early civilizations. The symbol "Au" comes from Latin word aurum, which is related to goddess of dawn, Aurora. Au is not very hard and it is one of the most ductile and malleable element in the world. It has very rich electrical conductivity. It is an inert metal and resistant to deformations by air, moisture and most chemicals. The inertness of Au makes it biocompatible. All these superior properties of Au make it very promising candidate for various applications.[61]

Nano-size Au shows special shape and size dependent optical properties. These properties are more pronounced for Au nanoparticles with non-spherical architectures and lead to many uses as sensing and imaging techniques, such as Surface Enhanced Raman Spectroscopy (SERS).

1.3.1. Some of the Applications of Gold Nanoparticles

1.3.1.1. Toxicity Detection

It is well known that heavy and transition metal ions are distributed widely in biological systems and environment. As a result, determination of toxic heavy metals is an important issue. [5] Due to extinction coefficient of Au nanorods, their longitudinal plasmon absorption can shift and this make them sensitive probe for sensing applications. This shift can be achieved by taking the advantage of affinity

between Au nanoparticles and toxic heavy metal ions.[62] For instance, heavy metal ions, like Mercury, can be detected with high sensitivity and selectivity.

1.3.1.2. Solar Cell

Investigation of renewable energy sources and increasing their efficiency are one of the main considerations of nowadays scientific community. Photovoltaic devices which convert the sunlight to the energy are attractive tools in utilization of renewable energy sources. Among all of photovoltaic devices, polymer based organic solar cells are under investigation since they have low cost of production, can be produced at room temperature, don't produce toxic gases and work quietly. Unfortunately, photon absorption efficiency of those materials is limited. As a result, their power conversion efficiency is affected from this situation negatively.[63,64] If device resistance wouldn't also increase, increasing thickness of active layer of organic solar cells may be a solution of this problem.[65–67] The addition of nanoparticles into layers of organic solar cells may increase LSPR effect and to reduce device resistance. Most of the research focused on this aim use spherical metal nanoparticles.[68–70] There are a few research based on using anisotropic nanoparticles in organic solar cells.[71] Among all of those nanoparticles, star shaped Au nanoparticles are the ones who show strongest contribution to the improvement on efficiency. It was expected because they have sharp features and strongest localized surface plasmon resonance.[4]

1.3.1.3. Optical Communication

The science and technology of communication at a distance by electronic transmission of impulses is known as telecommunication. Optical communication is any form of telecommunication that uses light as the transmission medium. Optical

waveguides is the most universal type of channels for optical communications.[6] An optical waveguide is a physical structure that guides electromagnetic waves in the optical spectrum. By attaching nanoparticles close to each other like chain, optical mode can be converted to non-radiating surface plasmon. Maier et al. reported that, transportation of electromagnetic energy from a localized sub-wave length source to a localized detector is provided. In this experiment a dye laser is used and by using fluorescent nanospheres the energy through the waveguide is functional end structures.[72,73]

1.3.1.4. Light Emitting Diodes

Light sources based on reliable and energy-efficient light-emitting diodes (LEDs) are instruments in the development of solid-state lighting. Surface plasmons were suggested as a way to enhance, light emission efficiency in LEDs.[74] Under the resonance condition localized surface plasmon effect enables metallic nanoparticle to capture the trapped light, enhancing the extracted efficiency of the light.[7] Jin et al. reported that, the optical output power of the LEDs was enhanced by employing Au nanoparticles. The enhancement was mainly originated from the surface plasmon effect and surface scattering effect from the Au nanoparticles. The optical output power of these LEDs was enhanced up to 55.3% for an input current of 100 mA.[7]

1.3.1.5. Biomedical Applications

Au nanoparticles have long body circulation times and strong absorption bands in NIR window. Moreover, their functionalization process is simple. Consequently, they can be used for drug delivery, contrasting agent and cancer therapy purpose.

Au nanorods that strongly scatter in the NIR region are able to detect cancer cells under excitation of spectral wavelength where biological absorption is lower.[8]

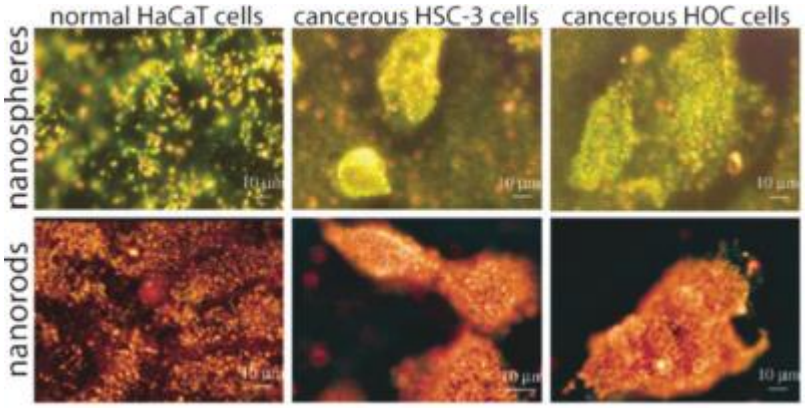

Figure 1.6. Cancer diagnostics using gold nanorod enhanced light scattering.[129]

Au nanoparticles can also be used in photothermal therapy. Photo thermal therapy is the way of destructing cancer cells by heating. Heat can be applied by various sources like radio frequencies, microwaves and lasers. Unfortunately, since tissues also absorb the heat, the amount of heat, which is expected to reach to cancer cell, is limited. When light absorbing materials inserted into the targeted cancer cell, cancer cells may absorb heat more efficiently.[5] As a result, tumor selectivity of this method can be improved. For example, El Sayed et al. conjugate Au nanorods to anti-EGFR antibodies. (Figure 1.6) By preferential binding of Au nanorods to human oral cancer cells, photothermal therapy could be used more efficiently. [8]

1.3.2. Synthesis of Gold Nanoparticles

Several methods have been used for the synthesis of Au nanoparticles up to date. Those methods can be classified in two main approach called as top-down and bottom-up. In top down approach, nanoparticles are prepared by making the size of materials from larger scale to nanoscale. One of the problems in top down approach is that it can cause damage or imperfections on the surface structure. Having expensive production tools and synthetic pathways is another negative side of this approach.[25,75] Lithography is one of the methods which which can be given as an example for top down approach.

Bottom up means that building large scale material by starting from the bottom, smaller ones. Bottom up approach comprise the mostly used methods in nanomaterial production. This approach gives the opportunity of having less defect and more homogeneous composition nanostructure.[75] Bottom up approach can also be divided as temple assisted and wet chemical methods. While electrochemical, photochemical, electroless method is counted as temple assisted methods, hydrothermal process, polyol process and seed mediated growth synthesis are counted as wet chemical methods. Detailed explanation of those methods will be given in the following sections.

1.3.2.1. Electrochemical Process

This method has been frequently used for noble metal nanoparticle production. In this method, nanoporous membrane template which is used for deposition of reduced metal ions under the applied voltage. In 1994, Reetz and Helbig showed that electrochemical process can be used for size-selective synthesis of nanoparticles by tuning current density [76] In this process while surfactant is electrolyte, stabilizer

is used as template.[77] The general scheme of the process is summarized in Figure 1.7.

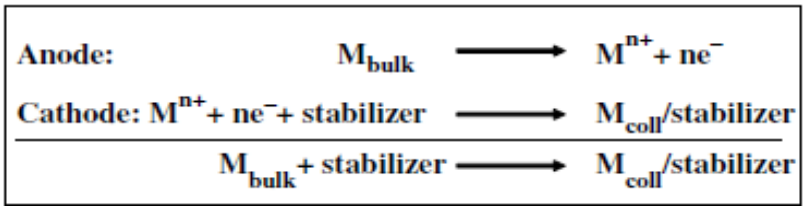

Figure 1.7. Scheme of electrochemical process.[76]

1.3.2.2. Electroless Process

"Electroless" plating is a term to describe the spontaneous reduction of metal ions to metallic particles and films in the absence of an external source of electric current. In the literature, electroless deposition is used as a term to define three different plating mechanisms. (Figure 1.8). Electroless deposition is applicable to a wide range of metal - substrate combinations.[78]

Electroless Method is classified according to reduction method of metal salts related to the role of surface in this process under three sub methods. In "Autocatalytic Electroless Process", reduced noble metals serve as the catalyst for further reduction of the salt by the external reducing agent. In "Substrate Catalyzed Electroless Process", substrate catalyzed deposition baths contain a metal salt and reducing agent. Metal reduction is facilitated on the substrate surface, and once completely coated, metal ions cease to be reduced from solution. In Galvanic Displacement,

there is no external reducing agent. The surface serves as an electron source for reduction of metal salt.[78]

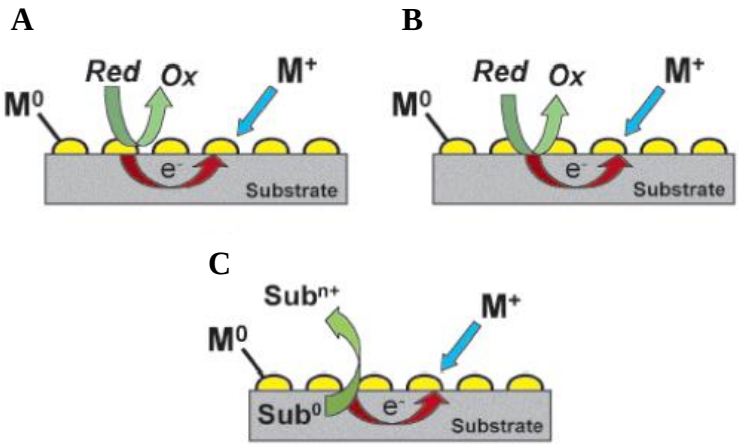

Figure 1.8. Electroless deposition process (A) Autocatalytic (B) Substrate Catalyzed (C) Galvanic Displacement. [78]

1.3.2.3. Photochemical Method

In this method, photoreduction of Au^{3+} to Au^{0} is accomplished by UV light. As in the seed mediated growth process, surfactant stabilizes specific face and leads the growth of anisotropic gold nanoparticles. Moreover, presence of Ag^{+} ion increase the aspect ratio and yield of nanoparticles formed.[79] Kim et al. reported that mostly spherical nanoparticles with a very small amount of gold nanorods are produced in the absence of $AgNO_3$. In their method, an apparent increase in the aspect ratio of gold nanorods was formed when more silver ion is added.[79] Photochemical reduction method requires long reaction time around 30 hours for the reduction of

Au^{3+} when there is no external reducing agent. On the other hand, this period can be decreased to 30 minutes if $HAuCl_4$ is first reduced by ascorbic acid and then exposed to UV radiation.[5] By using ketyl radicals like Irgacure-2959, rapid reduction of Au^{3+} to Au^0 occurs and gold nanorods are formed upon irradiation at 300 nm. [80,81]

1.3.2.4. Polyol Method

The polyol method involves the reduction of an inorganic salt by polyol, which refers to alcohols containing multiple hydroxyl groups, at an elevated temperature. By heating, ethylene glycol, can be converted to glycoaldehyde which is common reductant in polyol method.[25] Fievel[82] et al. and Viau et al.[83] reported that it is possible to make colloid particle of various shapes and sizes made of metals and their alloys by using polyol method.

1.3.2.5. Hydrothermal Method

Hydrothermal synthesis is generally defined as crystal synthesis or crystal growth under high temperature and high pressure water conditions from substances which are insoluble in ordinary temperature and pressure.[84] In this method water serves as not only catalyst but also component of solid phase. It is also possible to modify the characteristic of initial pure water.[25] Moreover, since polar solvents, acids, bases or apolar solvents can also be used, this method also named as solvothermal method.[85] This method has been used to synthesize various shapes of Au nanoparticles. For instance, E.Dertli et al. were able to synthesize Au nanowires with very high aspect ratios, structural purity, and yield by using modified hydrothermal method.[86]

1.3.2.6. Seed Mediated Method

This method has been first developed by Zsigmondy et al. and named as "nuclear" method.[5] About a century later, Jana et al. have improved the method and it was renamed as seed mediated growth method.[87] Nanoparticle growth in seed mediated method occurs in series of steps. The number of steps can be increased to obtain better control over size and shape of nanoparticles.[5] Seed mediated method includes two basic steps: i) formation of seeds and ii) growth of nanoparticles from those seeds. Briefly, the first step of the process include reduction of metal salt by strong reducing agent (i.e. $NaBH_4$) in the presence of surface directing agent (i.e Na-Citrate or Cetyltrimethylammoniumbromide (CTAB)).[88] In the second step seeds are added to a growth solution where more metal salt and surface directing agent present. The growth of nanostructures takes place with reduction of metal ions on seed surface.[5] The size shape and surface properties can be controlled by the concentration and nature of the reducing agent, surfactant and their ratio to metal salt. External agents like molecules or ions can also be used to manipulate the shape of nanoparticles.[25]

A seed-mediated method has many advantages over other bottom up methods. For instance, it allows controlling shape and size of nanoparticles by modifying both seeding and growth conditions. Moreover, this method provides possibility to monitor and understand growth mechanism of nanoparticles since it progress step by step. [89] The pH of reaction medium, reducing agent, and capping agent (surfactant) are some important factors in the synthesis and stabilization of metal nanoparticles. Also, the use of toxic reagents is minimized in the seed mediated method and this makes it more environmentally friendly and one of the green chemistry synthesis methods.[13]

The use of seed mediated method lead to synthesis of Au nanoparticles successfully in various morphologies. Some of the most commonly studied structures are summarized in following sections.

1.3.2.6.1. Seed Mediated Synthesis of Gold Nanospheres

Among all nanoparticle morphologies spherical ones are the most commonly studied ones. In 1950s Turkevich et al. reported the spherical Au nanoparticle synthesis route which is still being used today. In this method Au salt is reduced by sodium citrate, which is also acting as a stabilizing agent (surfactant) in aqueous media. (Figure 1.9) The Au nanoparticles which are synthesized with this method have sizes around 20 nm.[90] Later on larger Au nanoparticles have been synthesized by seed mediated growth where these 20 nm particles are used as seeds. Quite large number and variety of Au particles were reported by reduction with ascorbic acid by Goia and Matijevic.[91] Jana et al. have used the ascorbic acid reduction in the presence of citrate synthesized Au seeds and produce spherical Au nanoparticles in the size range of 20-100 nm.[92]

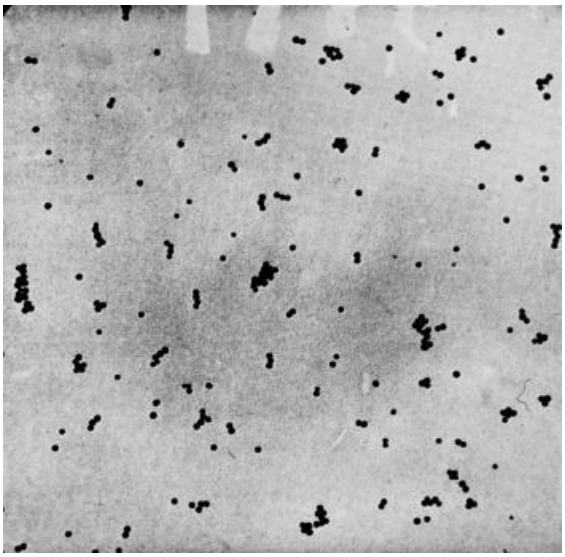

Figure 1.9. Electron migrograph of a gold nanoparticles synthesized with the reduction by sodium citrate.[90]

1.3.2.6.2. Seed Mediated Synthesis of Gold Nanorods

Au nanorods are other type of morphology which is found very interesting to study by researchers. This is mostly due to their exciting optical properties which lead them to be used in sensing and imaging applications. Also, their large surface areas provide a possibility of surface functionalization for various applications.

Synthesis of Au nanorods with seed mediated process is demonstrated with a schematic representation in Figure 1.10. Briefly, seed nanoparticles are being formed in the first step and these seeds are added into growth solution where the seeds are acting as nucleation sites and finally lead the growth of nanoparticles in rod shape.

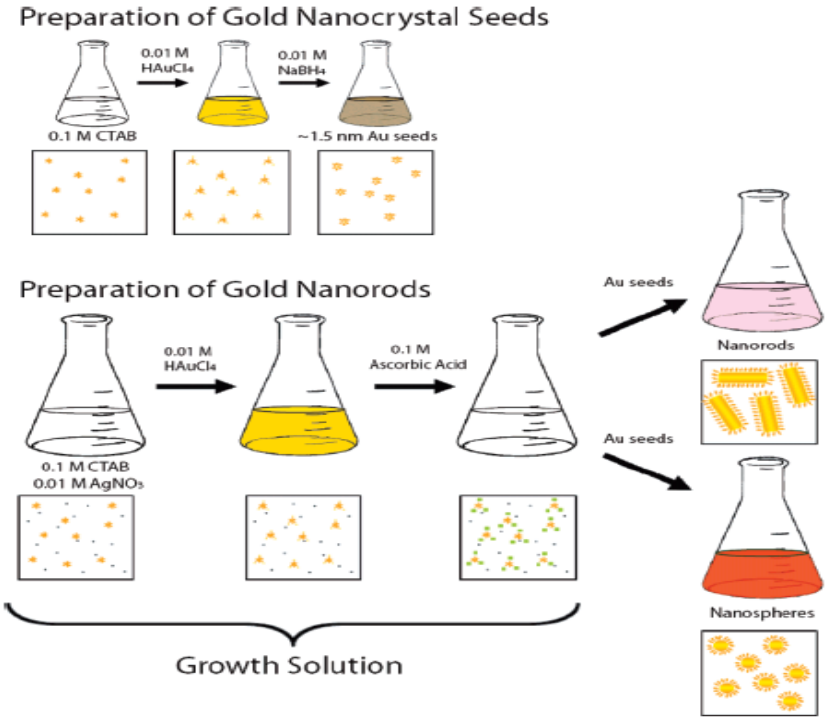

Figure 1.10. Seed-mediated surfactant-assistant gold nanorod synthesis.[130]

Important parameters such as concentration of reagents and their relative ratios, surfactant type, seed concentration, mixing order of chemicals have been investigated extensively to control the morphological features (i.e length or aspect ratios of nanorods. For instance, Murphy and co-workers have used CTAB as surfactant and introduced the use of $AgNO_3$ in the growth step as the citrate capped spherical nanoparticles were used as seeds.[87] They have observed that the use of CTAB substantially increased the nanorod yield.[93] El-Sayed and co-workers replace the citrate used in the seed formation step with CTAB and modified $AgNO_3$ concentration to control the aspect ratio of Au nanorods.[94] (Figure 1.11)

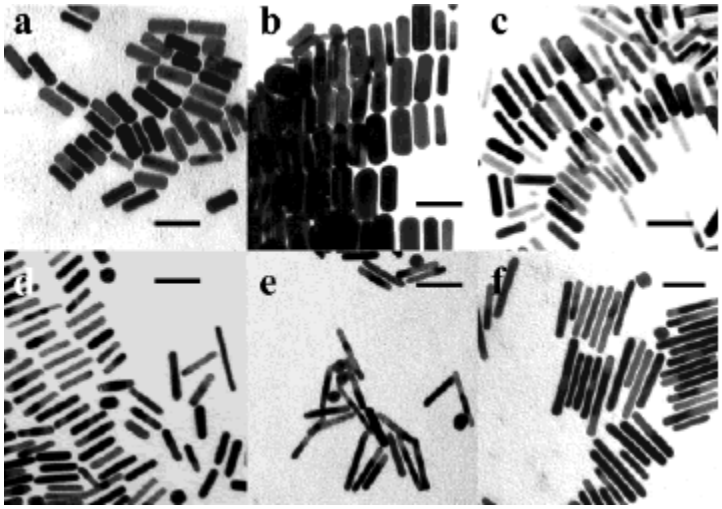

Figure 1.11. TEM images of gold nanorods.[94]

The use of CTAB as a surfactant has been breakthrough in the nanorod synthesis since it significantly improves the yield and provides a control over the aspect ratio of nanorods. Studies have been done to explain the mechanism of growth of nanorods directed by CTAB.[10,12,40,93,95,96] It has been reported that CTAB is preferentially bind to {100} face of nanocrystals and prevent the growth of nanoparticles on these faces. Blocking of these faces by CTAB lead the growth of nanoparticles from tips, on {111} faces.[10,12] The growth mechanism of nanorods is demonstrated schematically in Figure 1.12

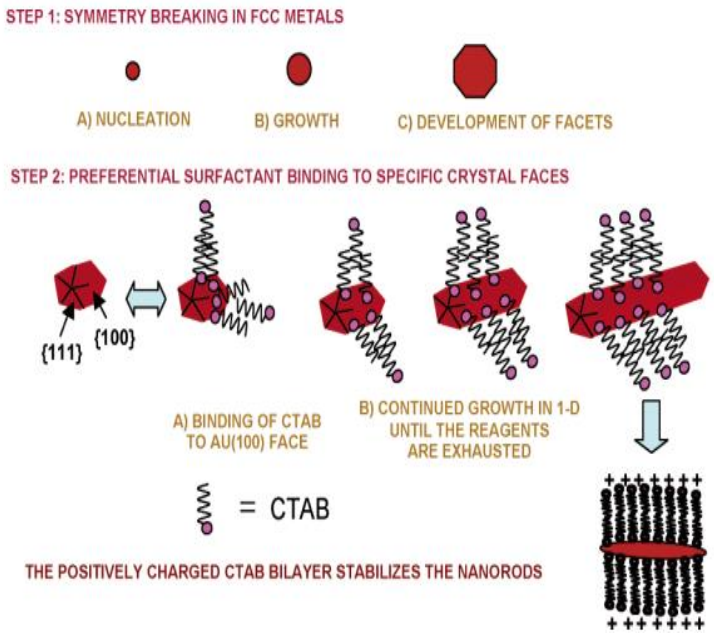

Figure 1.12. Schematic representation of surfactant directed growth of gold Nanorods.[11]

The role of $AgNO_3$ is almost crucial for the formation Au nanorods. Murphy et al. reported that in the presence of silver ion high yields of short nanorods are obtained while lower yields are obtained in the absence of silver.[12] It is proposed that $AgNO_3$ forms siver bromide (AgBr) layer in the presence of CTAB and those AgBr layers bind to {100} face of nanocrystals and lead the growth of nanoparticles from tips on {111} faces.[20,40] In addition to that, Guyot-Sionnest gave some useful insight into the role of silver and a possible rationale for the excess ions in solution. They found that Au nanorods grown using CTAB-protected Au seeds in the presence of Ag+ bear Au{110} faces on the sides of the rods and {100} faces on the ends.[97] Silver under potential deposition (UPD) is the reduction of Ag^+ to Ag^0 at a metal substrate with a surface potential less than the standard reduction potential of Ag^+. A greater positive shift in potential for silver UPD on Au surfaces is observed on {110}

surfaces compared to the {100} or {111} faces.[98] This suggests that deposition of silver on the sides of the rods ({110} facets) should be faster than on the ends that are {111}. Fast silver deposition followed by strong CTAB binding inhibits Au growth on the sides of the rods and leads to preferential growth of Au at the ends.[99]

1.3.2.6.3. Seed Mediated Synthesis of Branched Au Nanoparticles

Synthesis of Au nanorods steer the attention toward exploring new nanoparticles with anisotropic architectures due to their interesting optical which led them to sensing applications such as SERS.[9] These special optical properties of branched Au nanoparticles based on their high sensitivity to local changes in the dielectric environment, as well as formation of large electric field on the tips or sharp edges of the nanoparticles. [100]

Star[9,53,54], flower[55,101,102,3], urchin[103], tree shaped[104] structure are some of the examples of branched nanoparticles. (Figure 1.13) The synthesis of these nanostructures has been achieved by some modifications in the growth step of the seed mediated method. Change in the concentration of reactants and/or addition of chemicals such as NaOH to fasten the growth process yield the nanoparticles in branched structures. Even though exact mechanism of nanostar formation is not known, the reason for branching has been suggested as the formation of high defect density caused by rapid growth process. The poor binding of surfactant on these defect sites results in branching during growth of nanoparticles.[105]

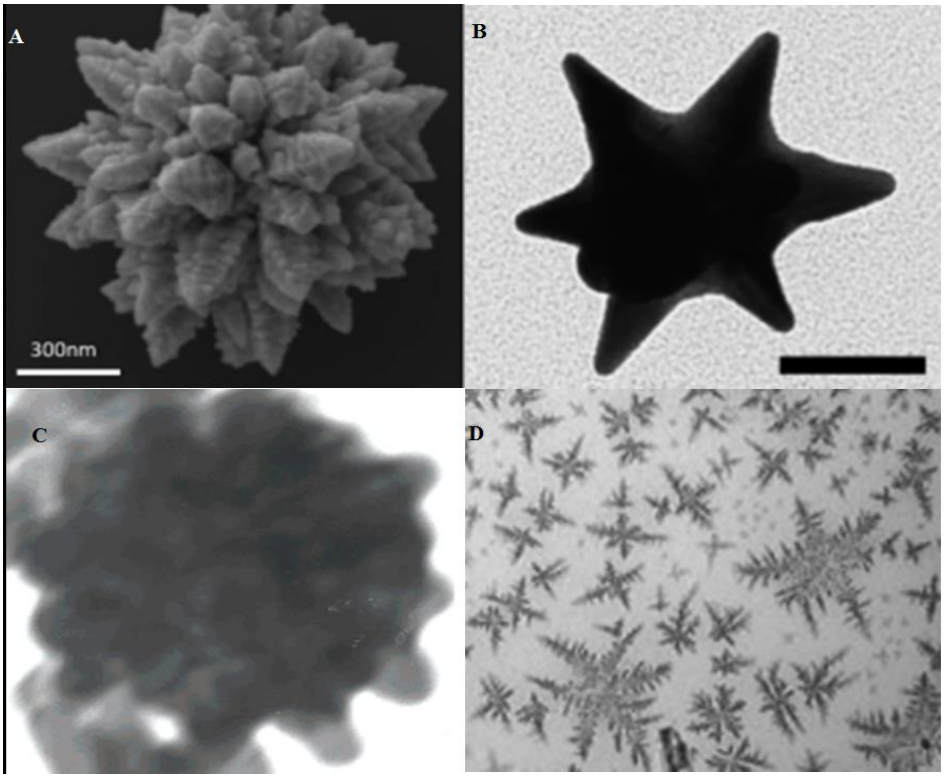

Figure 1.13. Images of branched gold nanoparticles. (A) Flower (B) Star (C) Urchin (D)Tree.[1,3,103,104]

1.3.3. Growth of Au Nanoparticles on Surfaces

Some of the applications of nanoparticles such as solar cell, catalysis, light emitting diodes and sensing requires fixing of particles on surfaces.[15] One way of achieving this is to adsorb nanoparticles on functionalized substrate surfaces via electrostatic or chemical interactions.[106,107, 108] Another alternative has been reported as growing nanoparticles directly on substrates.

Growth of Au nanoparticles on silicon and mica surfaces[14] or indium tin oxide (ITO) surfaces[15] by seed mediated method [93], have been reported. In these studies, firstly substrate surface is coated with a molecule to bind the seed particles on the

surface. Secondly, the seed particles have been attached on the functionalized surface. Finally, the seed-attached surface is placed in growth solution to allow the synthesis of nanoparticles on the surface

The bridging molecules chosen have two functional groups; one has affinity toward Au such as –SH and $–NH_2$ and the other prefer attaching to the hydroxyl/oxide groups on the substrate such as alkoxy silane.[109–111,112]. The use of two molecules; 3-mercaptopropyl-trimethoxysilane (MPTMS) and 3-aminopropyl-trimethoxysilane (APTMS) have been reported for this purpose.[112] It is proposed that those functional groups on the surface may interact with Au(0) formed during the reduction of $AuCl_4^-$ when growing around the seed particles in the growth solution. As a result it is expected that silane growing parts of Au can attach or connect with the functional groups on the surface. [15]

Taub and co-workers have aimed to synthesize Au nanorods on silicon and mica surfaces. In their study, they have first coated the surface with APTMS and then immersed it into the seed solution to capture the seeds on the surface. Finally, incubating the seed coated surface in CTAB solution for some period of time and in $HAuCl_4$ and ascorbic acid added solution yielded Au nanorods as well as Au nanoparticlew in different morphologies.[14] (Figure 1.14)

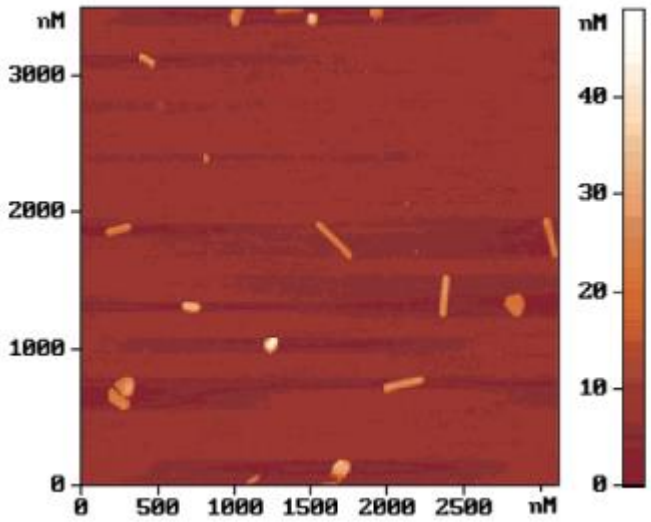

Figure 1.14. AFM Image of the grown gold particles on mica.[14]

In another study by Kambayashi and co-workers, Au nanoparticles have been synthesized and ITO coated glass surface.[15] In this study, similar approach to the Taub's study has been followed except that the use of different bridging molecule; MPTMS instead of APTMS. Figure 1.15 demonstrates the SEM image of Au nanoparticles synthesized in this study.

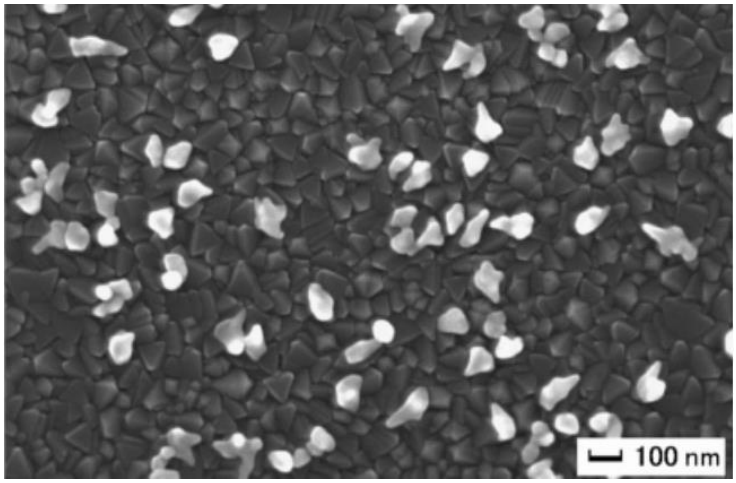

Figure 1.15. FE-SEM image of the gold nanoparticles on MPTMS modified ITO surface.[15]

A few studies have been reported on synthesis of Au nanoparticles on surfaces. As it is seen from the examples given above, nanoparticles have formed in mixture of morphologies and in low yield. To our knowledge, there is no study reported on modifying parameters to obtain high yield and structural purity for the nanoparticle synthesis on surfaces, yet.

CHAPTER 2

EXPERIMENTAL

2.1. Chemicals

L-Ascorbic acid, silver nitrate ($AgNO_3$), hydrogen tetrachloroaurate (III) trihydrate ($HAuCl_4.3H_2O$), sodium hydroxide ($NaBH_4$), (3-aminopropyl)-trimethoxysilane (APTMS) and toluene were purchased from Sigma –Aldrich; trisodium citrate dihydrate, sodium borohydride ($NaBH_4$), sulfuric acid (H_2SO_4) and hydrochloric acid (HCl) were purchased from Merck; cetyltrimethylammoniumbromide (CTAB) was purchased from Fluka and used without further purification. 10 nm Au colloids were purchased from Ted Pella. ITO film-coated glass was purchased from Delta Technologies (20Ω, size ca 7x50x0.7 mm). All experiments were conducted at room temperature. As solvent, ultrapure deionized water (resistivity greater than 18 MΩ) is used for all solutions.

2.2. Characterization

Scanning electron microscopy (SEM) studies were acquired using FEI Nova Nano SEM 430 microscope and QUANTA 400F Field Emission SEM. X-ray diffraction (XRD) measurements were done on a Rigaku D Miniflex pc diffractometer with Cu Kα radiation (λ = 1.54 Å) operating at 30 kV. Also, a Varian model Cary 100 Bio UV-Vis spectrophotometer within the wavelength range of 190-1000 nm was used to observe formation of NPs.

2.3. Synthesis of Nanostars on Surfaces

In this study, synthesis of branched nanoparticles was achieved on three different surfaces (silicon wafer, ITO coated glass and glass). Synthesis include three main steps: i) preparation of the surfaces by functionalizing them with APTMS, ii) adsorption of seed nanoparticles on the surfaces, and iii) growth of nanostars by placing seed attached surfaces in growth solutions. In the following sections growth solutions are described, and finally experimental details of steps for branched nanoparticle synthesis on surfaces are given.

2.3.1. Preparation of Seed Solutions for the Synthesis of Nanostars on Surfaces

2.3.1.1. Preparation of Gold Nanospheres

Au nanospheres were prepared in three different sizes (4, 8 and 15 nm) as described in literature.[96]

2.3.1.1.1. Preparation of ca 4 nm Gold Seeds

In the synthesis of 4 nm Au nanospheres, firstly all reactants are mixed in a 15 mL polypropylene centrifuge tube in the following order:

- 9.50 mL ultrapure Water
- 0.25 mL, 0.01 M, $HAuCl_4$ solution
- 0.25 mL, 0.01 M , sodium citrate solution

Mixing the solutions given above followed by addition of 0.30 mL, freshly prepared and ice-cold, 0.1 M $NaBH_4$ and the final solution was mixed rapidly by using

vortex for two minutes. The cup of the vial was opened periodically to release the hydrogen gas formed. The color of solution turned pale brown indicating the formation of spherical nanoparticles. The mixture was kept undisturbed at 27°C for three hours in water bath.

2.3.1.1.2. Preparation of ca 8 nm Gold Sphere

In the synthesis of ca. 8 nm Au nanospheres ca. 4 nm nanoparticles were used as seeds. The synthesis starts with addition of reactants in the following order:

- 45 mL, 0.08 M, CTAB solution
- 1.125 mL, 0.01 M, $HAuCl_4$ solution
- 0.25 mL, 0.1 M freshly prepared ascorbic acid solution

The color of the solution becomes yellow-orange with the addition of $HAuCl_4$ into the CTAB. Addition of ascorbic acid made the solution indicating reduction of Au^{3+} ions to Au^{+}. Lastly, 5 mL ca. 4 nm nanospheres were added to start the growth of ca. 8 nm nanospheres. The final mixture was stirred vigorously by using vortex for 10 minutes. The solution was kept undisturbed at 27°C for three hours in water bath.

2.3.1.1.3. Preparation of ca. 15 nm Gold Sphere

Spherical nanoparticles (ca.8 nm) prepared in the previous step were used as seeds in the synthesis of ca. 15 nm Au nanospheres. Similarly, here CTAB, $HAuCl_4$ and ascorbic acid were mixed in an order given below.

- 45 mL, 0.08 M, CTAB solution
- 1.125 mL, 0.01 M, $HAuCl_4$ solution

- 0.25 mL, 0.1 M, freshly prepared ascorbic acid solution

Similar to the 8 nm nanosphere synthesis, after the addition of ascorbic acid and observing the color of the solution turn yellow-orange to colorless 5 mL seed solution (ca. 8 nm spheres) were added. The final mixture was stirred vigorously by using vortex for 10 minutes. The solution was kept undisturbed at 27°C for three hours in water bath.

2.3.1.2. Preparation of Gold Nanorods

Nanorods with ca.4 aspect ratio were synthesized by mixing all reactants in the following order:

- 4.15 mL ultra-pure water
- 0.4 mL, 0.01 M, $HAuCl_4$ solution
- 4.75 mL, 0.2 M, CTAB solution
- 0.06 mL, freshly prepared 0.01 M $AgNO_3$
- 0.64 mL, freshly prepared 0.01 M ascorbic acid

After gentle mixing, the 2 hours aged, CTAB stabilized 31.25 µL seed solution is added to this growth solution. The solution was mixed gently. The solution was kept undisturbed at 27°C for two hours in water bath.

2.3.1.3. Preparation of Gold Nanostars

Nanostar synthesis was achieved by using commercially available 10 nm spherical gold colloid as seeds. Growth solution for nanostars was prepared by mixing the reactants in the order given below:

- 4.75 mL, 0.1 M, CTAB solution
- 0.2 mL, 0.01 M, $HAuCl_4$ solution
- 0.03 mL, freshly prepared 0.01 M $AgNO_3$
- 0.032 mL, freshly prepared 0.1 M ascorbic acid

10 nm Au colloid seed is added to growth solution and mixed gently. The solution was kept undisturbed at 27°C for two hours in water bath.

2.3.2. Preparation of Growth Solutions

In this study, three different growth solutions were prepared to monitor changes in the morphologies of products and to find optimum concentrations of reactants for best quality (uniform size and shape) products possible. These growth solutions are the ones used in the synthesis of nanostars, nanorods and nanospheres, and labelled as growth solution A, B and C, respectively. The growth solutions differ in concentrations of reactants (i.e. CTAB, $HAuCl_4$, $AgNO_3$, ascorbic acid) used. The solutions are described in the following sections.

2.3.2.1. Preparation of Growth Solution A

Growth solution A is originally used to synthesize nanostar colloid. [9] Here, in this part of the study it was used as a media to grow nanoparticles on surfaces. The solution was prepared by mixing reactant in the following order:

- 4.75 mL, 0.1 M, CTAB solution
- 0.2 mL, 0.01 M, $HAuCl_4$ solution
- 0.03 mL, freshly prepared 0.01 M $AgNO_3$
- 0.032 mL, freshly prepared 0.1 M ascorbic acid

As described before, the addition of ascorbic acid turn the color of the solution from yellow-orange to colorless indicating reduction of Au^{3+} ions.

2.3.2.2. Preparation of Growth Solution B

Growth solution B is reported to synthesize nanorod colloid.[42] The solution was prepared by mixing reactants with given concentrations and amounts below for the growth of nanoparticles on surfaces.

- 4.15 mL ultra-pure water
- 0.4 mL, 0.01 M, $HAuCl_4$ solution
- 4.75 mL, 0.2 M, CTAB solution
- 0.06 mL, freshly prepared 0.01 M $AgNO_3$
- 0.64 mL, freshly prepared 0.01 M ascorbic acid

2.3.2.3. Preparation of Growth Solution C

Growth solution C is reported to synthesize sphere colloid.[96] In this study, it was prepared to synthesize nanoparticles on surfaces by mixing reactants in the following order:

- 45 mL, 0.08 M, CTAB solution
- 1.125 mL, 0.01 M, $HAuCl_4$ solution
- 0.25 mL, 0.1 M, freshly prepared ascorbic acid solution

As described before, the addition of ascorbic acid turn the color of the solution from yellow-orange to colorless indicating reduction of Au^{3+} ions.

2.3.3. Preparation of Substrate Surfaces for Adsorption of Seeds

2.3.3.1. Cleaning Procedure

Substrates (Si-wafer and glass) were kept in 95-98 % sulfuric acid (H_2SO_4) for about one hour. Then they were washed with ultrapure water thoroughly. Finally, they were dried under nitrogen (N_2) gas.

2.3.3.2. Functionalization of Surfaces with APTMS

The functionalization of surfaces with APTMS was performed by following a method reported in literature.[14] Clean substrates were treated with 0.01 % toluene solution of APTMS for 30 minutes. Then substrates were washed with ethanol and ultrapure water. For drying, N_2 gas was used at the end of the process.

2.3.4. Adsorption of Seeds and Growth of Nanoparticles on Surfaces

Adsorption of nanoparticles used as seeds onto the surfaces was achieved by immersing APTMS functionalized substrates into seed solutions and incubating them for 3 hours at room temperature. Later, substrates were removed from seed solution, washed with ultra-pure water several times and dried with a flow of N_2 gas.

Synthesis of nanoparticles was performed by placing seed coated substrates into the previously prepared growth solutions. The substrates were kept in these solutions undisturbed for 24 hours, at 27°C.

In this study, parameters such as seed type (sphere, rod, star), seed size (for spherical nanoparticles; 4, 8 and 15 nm), concentration of reactants (use of different

growth solutions) and pH of the growth solution were investigated. As prepared growth solutions had a pH value about 3. This value was increased or decreased with the addition of NaOH and HCl to the growth solution, respectively. The concentration and amount of NaOH and HCl used, pH values obtained upon these additions and overview of other parameters investigated are given in Table 2.1

Table 2.1. Sets of experiments were performed in the parametric investigation.

Seed Solution	Growth Solution	pH of Medium
4 nm Sphere	Growth Solution A	*1.43 (300μL-1.0 M HCl)*
4 nm Sphere	Growth Solution B	*1.40 (300μL-1.0 M HCl)*
4 nm Sphere	Growth Solution C	*1.47 (300μL-1.0 M HCl)*
4 nm Sphere	Growth Solution A	*2.96 (No Addition)*
4 nm Sphere	Growth Solution B	*2.99 (No Addition)*
4 nm Sphere	Growth Solution C	*3.10 (No Addition)*
4 nm Sphere	Growth Solution A	*6.36 (102μL-0.1M NaOH)*
4 nm Sphere	Growth Solution B	*6.46 (102μL-0.1M NaOH)*
4 nm Sphere	Growth Solution C	*6.25 (55μL-0.1M NaOH)*
4 nm Sphere	Growth Solution A	*11.01 (250μL-0.1M NaOH)*
4 nm Sphere	Growth Solution B	*10.95 (250μL-0.1M NaOH)*
4 nm Sphere	Growth Solution C	*11.28 (250μL-0.1M NaOH)*
8.0 nm Sphere	Growth Solution A	*1.40 (300μL-1.0 M HCl)*
8.0 nm Sphere	Growth Solution B	*1.42 (300μL-1.0 M HCl)*
8.0 nm Sphere	Growth Solution C	*1.45 (300μL-1.0 M HCl)*
8.0 nm Sphere	Growth Solution A	*2.83 (No Addition)*
8.0 nm Sphere	Growth Solution B	*2.72 (No Addition)*

Table 2.1. (Continued)

Seed Solution	Growth Solution	pH of Medium
8.0 nm Sphere	Growth Solution C	*3.13 (No Addition)*
8.0 nm Sphere	Growth Solution A	*7.53 (102μL-0.1M NaOH)*
8.0 nm Sphere	Growth Solution B	*6.84 (102μL-0.1M NaOH)*
8.0 nm Sphere	Growth Solution C	*7.11 (55μL-0.1M NaOH)*
8.0 nm Sphere	Growth Solution A	*11.0 (250μL-0.1M NaOH)*
8.0 nm Sphere	Growth Solution B	*10.97 (250μL-0.1M NaOH)*
8.0 nm Sphere	Growth Solution C	*11.15 (250μL-0.1M NaOH)*
15.0 nm Sphere	Growth Solution A	*1.44 (300μL-1.0 M HCl)*
15.0 nm Sphere	Growth Solution B	*1.42 (300μL-1.0 M HCl)*
15.0 nm Sphere	Growth Solution C	*1.46 (300μL-1.0 M HCl)*
15.0 nm Sphere	Growth Solution A	*2.84 (No Addition)*
15.0 nm Sphere	Growth Solution B	*2.87 (No Addition)*
15.0 nm Sphere	Growth Solution C	*3.08 (No Addition)*
15.0 nm Sphere	Growth Solution A	*7.94 (102μL-0.1M NaOH)*
15.0 nm Sphere	Growth Solution B	*7.42 (102μL-0.1M NaOH)*
15.0 nm Sphere	Growth Solution C	*7.34 (55μL-0.1M NaOH)*
15.0 nm Sphere	Growth Solution A	*10.97 (250μL-0.1M NaOH)*

Table 2.1. (Continued)

Seed Solution	Growth Solution	pH of Medium
15.0 nm Sphere	Growth Solution B	*10.93 (250μL-0.1M NaOH)*
15.0 nm Sphere	Growth Solution C	*11.18 (250μL-0.1M NaOH)*
Rod	Growth Solution A	*1.45 (300μL-1.0 M HCl)*
Rod	Growth Solution B	*1.48 (300μL-1.0 M HCl)*
Rod	Growth Solution C	*1.45 (300μL-1.0 M HCl)*
Rod	Growth Solution A	*2.92 (No Addition)*
Rod	Growth Solution B	*2.92 (No Addition)*
Rod	Growth Solution C	*3.10 (No Addition)*
Rod	Growth Solution A	*6.46 (102μL-0.1M NaOH)*
Rod	Growth Solution B	*7.23 (102μL-0.1M NaOH)*
Rod	Growth Solution C	*7.15 (55μL-0.1M NaOH)*
Rod	Growth Solution A	*11.10 (250μL-0.1M NaOH)*
Rod	Growth Solution B	*11.24 (250μL-0.1M NaOH)*
Rod	Growth Solution C	*11.51 (250μL-0.1M NaOH)*
Star	Growth Solution A	*1.44 (300μL-1.0 M HCl)*
Star	Growth Solution B	*1.47 (300μL-1.0 M HCl)*
Star	Growth Solution C	*1.46 (300μL-1.0 M HCl)*

Table 2.1. (Continued)

Seed Solution	Growth Solution	pH of Medium
Star	Growth Solution A	*2.99 (No Addition)*
Star	Growth Solution B	*2.84 (No Addition)*
Star	Growth Solution C	*3.00 (No Addition)*
Star	Growth Solution A	*6.80 (102µL-0.1M NaOH)*
Star	Growth Solution B	*7.68 (102µL-0.1M NaOH)*
Star	Growth Solution C	*7.36 (55µL-0.1M NaOH)*
Star	Growth Solution A	*11.00 (250µL-0.1M NaOH)*
Star	Growth Solution B	*10.98 (250µL-0.1M NaOH)*
Star	Growth Solution C	*10.98 (250µL-0.1M NaOH)*

CHAPTER 3

RESULTS & DISCUSSION

In this study, synthesis of Au nanoparticles with branched morphologies were achieved on three different substrate surfaces; Si wafer, glass and ITO. The schematic representation of synthesis route is demonstrated in Figure 3.1. The process has three main steps: i) functionalization of the substrate surface, ii) chemisorption of gold seeds on functionalized surface, and iii) growth of branched nanoparticles on surfaces.

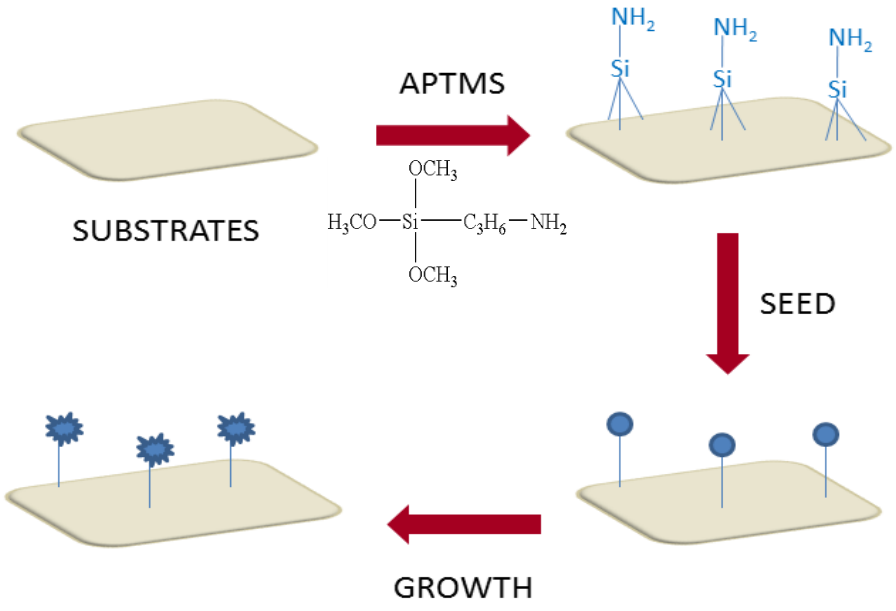

Figure 3.1. Schematic representation of growth of branched Au nanoparticles on surfaces. Inset shoows the structure of APTMS.

In the first step of the process, the substrate surfaces were coated with a molecule, (3-Aminopropyl)trimethoxysilane (APTMS) which act as a bridge between surface and Au nanoparticle. APTMS has two end groups; silanol and amine. As silanol group preferentially attach to the substrate surface, amine group interact with Au and finally link between surface and Au particle is established.[15,112] The last two steps of the procedure are based on seed mediated method with an exception of growing nanoparticles on surfaces instead of in solution.[14,15,93] Finally, Au seed coated surfaces were washed to remove seed particles which were not bind to the surface and incubate the coated substrate in growth solution for certain amount of time. The growth of nanoparticle on glass and ITO substrate were monitored with the change in the color of surface. It changes from colorless to purple. On the other hand, the nanoparticle growth made the shiny surface of Si wafer matte. Moreover, not observing any color change in growth solution indicates that either there is no growth of nanoparticles in solution or they form in very insignificant amount. Detecting no absorption band in UV-Vis measurements verify this observation. (Figure A1 in Appendices) This suggests that seed nanoparticles attached on surface strongly and they do not leave the surface during growth process.

Similar procedure has been followed by Kambayashi et al.[15] and Taub et al.[14] to synthesize rod and spherical shaped nanoparticles on surfaces. In these studies, different morphology of nanostructures was obtained as well the desired ones (rod shaped) which were formed in very low yield. Also, in these studies the investigation on improving structural uniformity and yield were not reported. In our work, however, the process were modified and parameters such as seed type, seed size and growth media (concentration of reactants and pH of the solution) were investigated thoroughly to obtain branched nanoparticles in high yield and structural purity (Figure 3.2.). Moreover, the synthesis of these particles on different surfaces was achieved under optimum conditions which are determined after a parametric study. Parametric study investigation was performed on Si-wafer surface since it

does not require any conductive material coating and thus makes monitoring particles with Scanning Electron Microscopy (SEM) more practical.

The characterization of synthesized nanostructures was performed by SEM, X-Ray Diffraction (XRD) and Energy Dispersive X-ray (EDX) studies. In the following sections of this chapter the results of i) synthesis at optimum experimental conditions on Si-wafer surface, ii) parametric study performed to determine the optimum conditions on Si-wafer surface, and iii) branched nanoparticle synthesis on ITO and glass substrate surfaces and their comparison with the ones on Si-wafer are discussed.

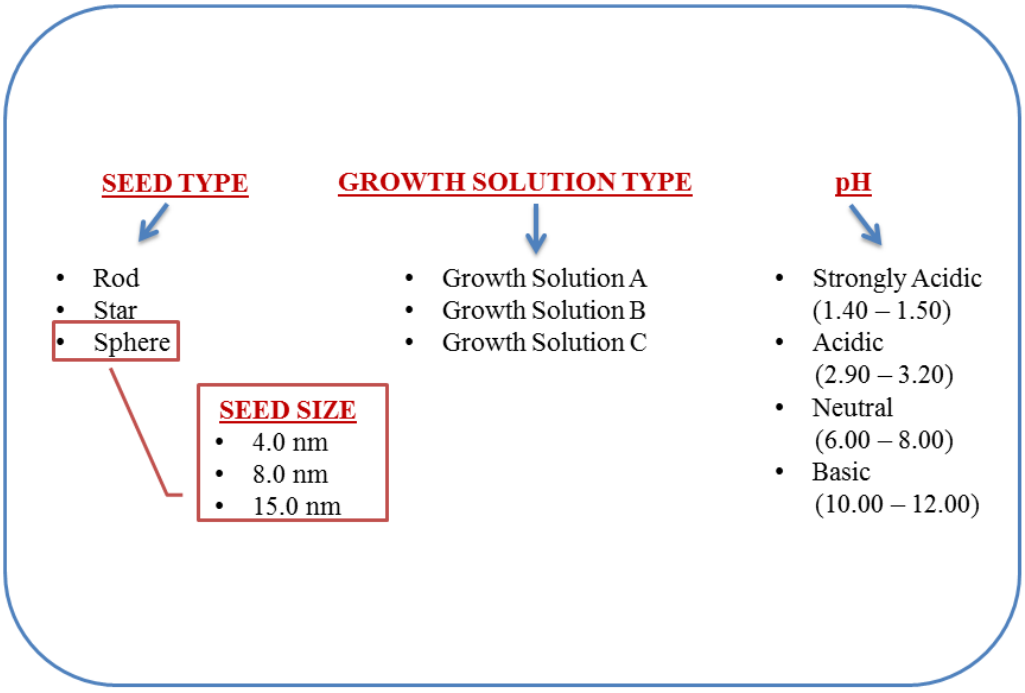

Figure 3.2. Summary of parametric study for the synthesis of branched Au nanoparticles on Si-wafer surfaces.

3.1. Synthesis of Branched Gold Nanoparticles on Si-Wafer Surfaces

3.1.1. Synthesis of Branched Gold nanoparticles at Optimum Experimental Conditions

The optimum conditions to synthesize branched Au nanoparticles in high morphological purity and yield were determined by the investigation of reaction parameters (i.e. seed type, seed size and growth media). This investigation revealed that the use of 8 nm Au nanospheres as seeds and growth solution (labelled as A) with 0.1 M CTAB, 0.01 M $HAuCl_4$, 0.01 M $AgNO_3$, 0.1 M ascorbic acid and pH of ca. 3 yielded the desired nanostructures.

Figure 3.3 shows SEM image of seed nanoparticles (ca. 8 nm Au nanospheres) which are chemisorbed on APTMS coated Si-wafer substrate. The image verifies that the chemisorption of seed nanoparticles on to the surface was achieved successfully.

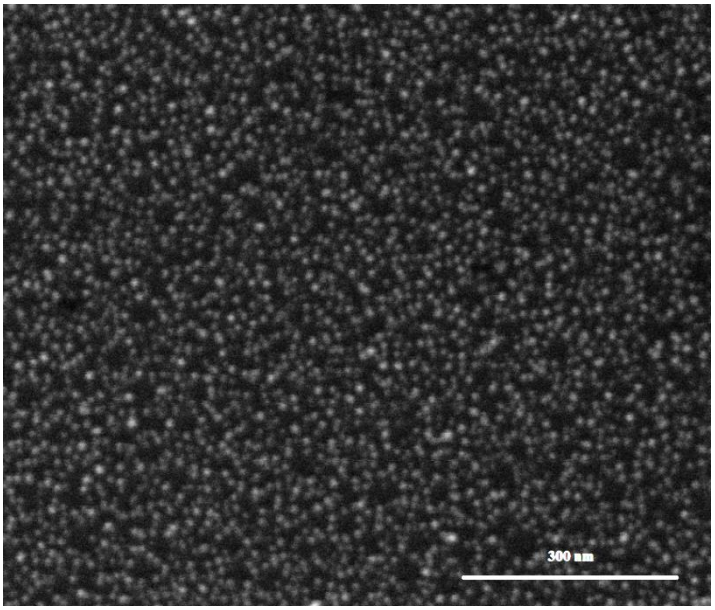

Figure 3.3. SEM image of ca. 8 nm spherical gold nanoparticles chemisorbed on APTMS coated Si-wafer.

SEM images of branched Au nanoparticles synthesized at optimum conditions on Si-wafer surfaces are given in Figure 3.4. The nanostructures have three dimensional morphologies with different numbers of sharp tips grown out of the nanoparticle core. SEM analysis revealed that all nanostructures synthesized at optimum conditions have branched morphology with average sizes (tip-to-tip) distance is about 450 nm. Even though synthesized nanostructures do not have uniform shapes due to differences in tip lengths, not observing particles with other structures suggest the synthesis of nanoparticles was achieved in high structural purity.

The SEM analyses show significant number of nanoparticles was remained on the surface even after multiple washing processes to remove unreacted reagents and/or non-bonded particles. This suggests strong attachment of branched Au nanoparticles

to the surface during and after the growth of nanostructures. This attachment is most likely due to the interaction between amine groups of the linker molecule (APTMS) and the Au nanoparticles. Initially Au-amine is formed between the Au(0) produced from the reduction of $AuCl_4^-$ when growing around the seed particles in the growth solution. Then, growing parts of Au nanostructures build new interactions with the ammine groups on the functionalized surfaces, thus stronger attachment of nanostructures to the surface can be achieved. [15] The EDX data verify the elemental identity of synthesized branched nanostructures as Au as expected.

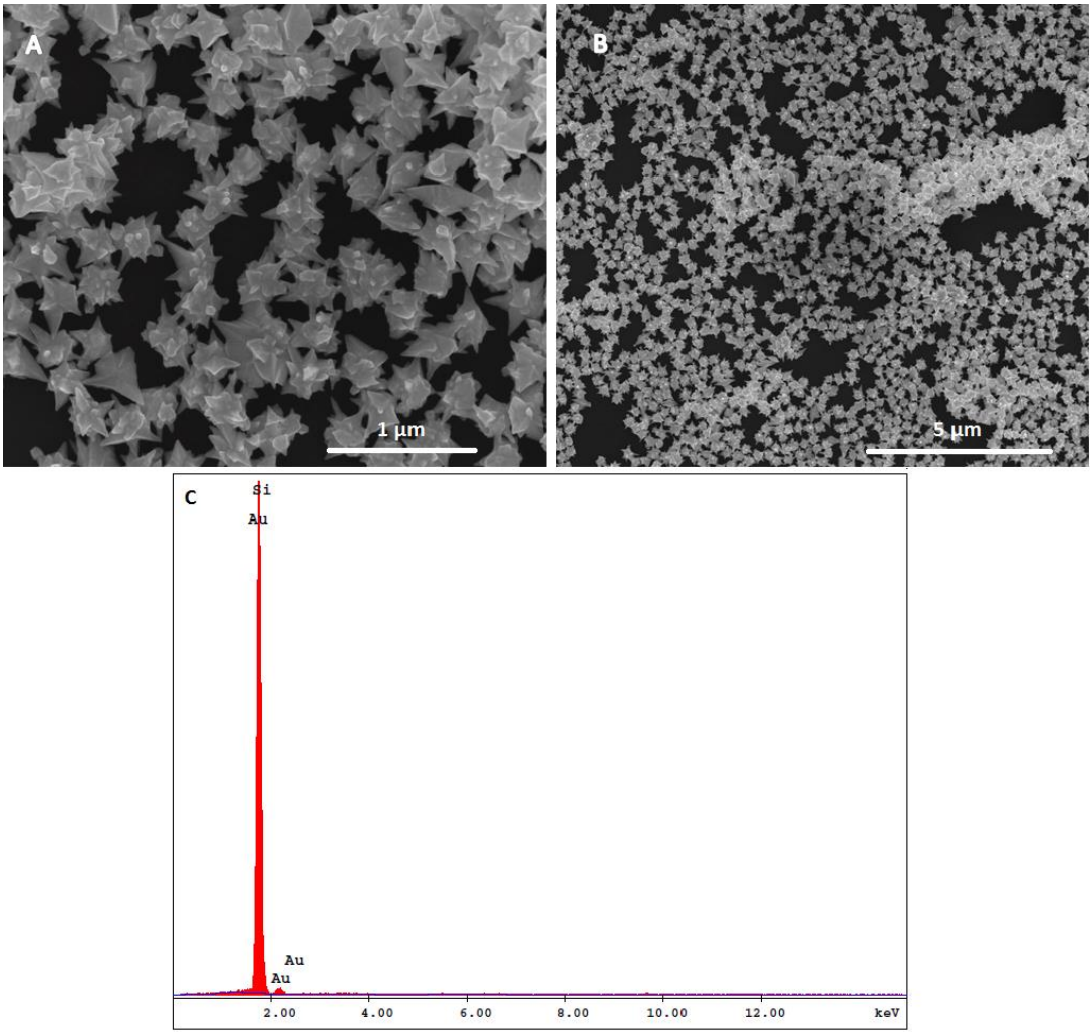

Figure 3.4. Figure A and B shows SEM images of branched gold nanoparticles on Si-wafer surfaces at different magnifications. Figure C shows EDX spectrum of those particles.

XRD analysis confirmed the crystal structure of branched Au nanoparticles. Figure 3.5 illustrate XRD patterns of branched Au nanoparticles synthesized on Si-wafer at optimu”m reaction conditions. However, the results show some Au diffraction peaks of Au (i.e. at 2Θ: 38.37° , 44.56°) are hindered by the ones of Si. The subtraction of

Si wafer XRD data from the ones collected from Au nanoparticle coated Si wafer ones reveal some of the diffraction peaks that belong to the Au nanoparticles. (Figure 3.5.A) The peaks observed for Au nanostructures (at 2Θ: 38.37°, 44.56°, 61.98°, 69.41°) were indexed to (111), (200), (220) and (311) planes of face-centered cubic (fcc) Au, respectively (JCPDS Card No. 65-2870).[113]

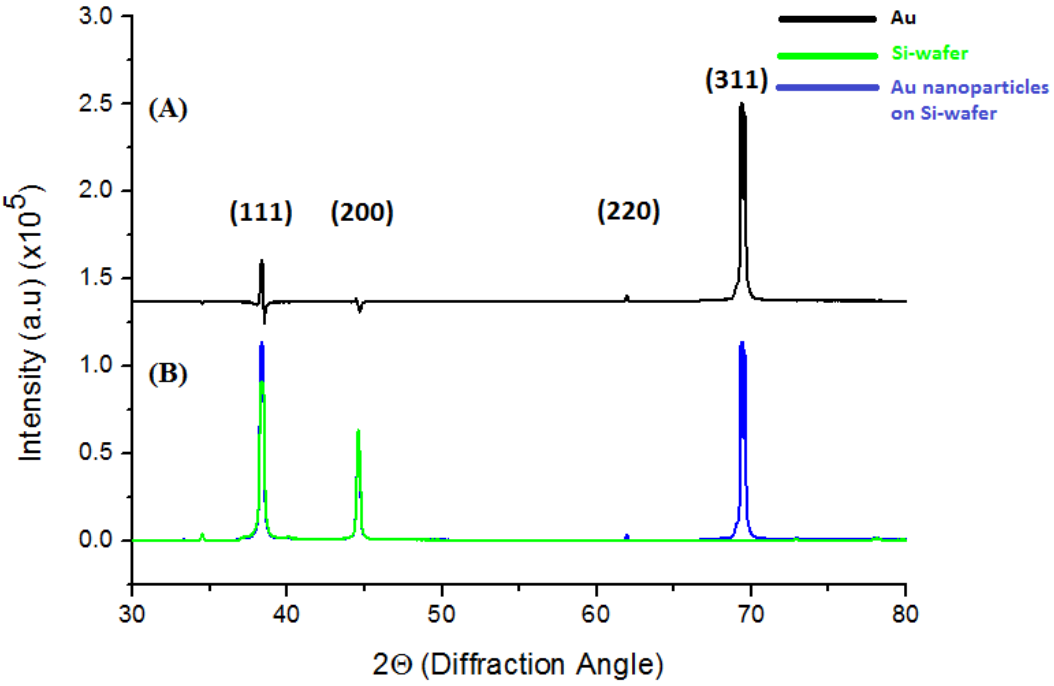

Figure 3.5. XRD pattern of A) Si-wafer (green) and branched gold nanoparticles on Si-wafer surfaces (blue), B) gold nanoparticles (NPs) which is obtained by substracting XRD data of Si-wafer from the ones of gold nanoparticle chemisorbed on Si-wafer (black).

3.1.2. Investigation of Parameters in the Synthesis of Branched Gold Nanoparticles on Si-wafer Surface

In this work, parameters such as seed type, seed size and growth media (concentration of reactants and pH of the solution) were investigated to decide on the best possible experimental conditions to synthesize branched Au nanoparticles in high yield and structural purity. In this investigation, 60 different combinations of parameters have been studied and each set of combination was repeated multiple times to make sure the obtained results are reliable and reproducible. The sets of combinations studied are listed in the Table 2.1. Hundreds of SEM images have been thoroughly examined to report the most reliable results possible. The results of this extensive investigation are summarized in the following sections. In each section, the results are compared for different sets of parameter combinations where only one parameter was changed as the others were kept same.

3.1.2.1. Effect of the Size of Spherical Nanoparticles as Seeds

In all of the synthesis methods of bottom-up approach, seed characteristics such as size and shape have determining role on the structural properties of nanoparticles produced. Manipulations of these characteristics provide the possibility of tuning the morphologies and many other important properties to obtain the desired nanomaterials for particular application.

In this part of the study three different sizes of spherical nanoparticles were used as seeds to investigate their effect on the quality of nanostructures formed. Other parameters like reactant concentrations and pH of the growth solution were kept same in each set of the experiment to observe the seed size effect more clearly. The growth solution used (labelled as Growth Solution A) contain the appropriate

concentrations of reactants to synthesize star shaped nanoparticles as described in literature.[9] The pH of the growth solution was kept around 3.

Figure 3.6. illustrate the change in the structural properties of the synthesized nanostructures as different sizes of seeds are used. Comparison of these SEM images at same magnifications indicates that smaller particles were grown from the smaller seed particles as expected. The nanostructures grown from the 4, 8 and 15 nm seeds have average sizes ca. 290, 450 and 760 nm, respectively. This is most likely due to the increase in the overall surface to volume ratio as the size of seed particle decrease, thus decrease in the amount of gold ions in solution per particle surface area. As a result of this, less number of Au^{+} ions is reduced on the each seed particle surface to grow them into larger nanostructures. In general, growth of nanoparticles in larger sizes can also be associated with a secondary growth process called as Ostwald ripening and defocusing.[114] In this process, particles which are smaller than the critical size dissolve and contribute to the growth of larger ones. Thus, larger particles grow into even larger ones. This might be the other possible reason to observe the formation of larger structures as the seed size get larger.

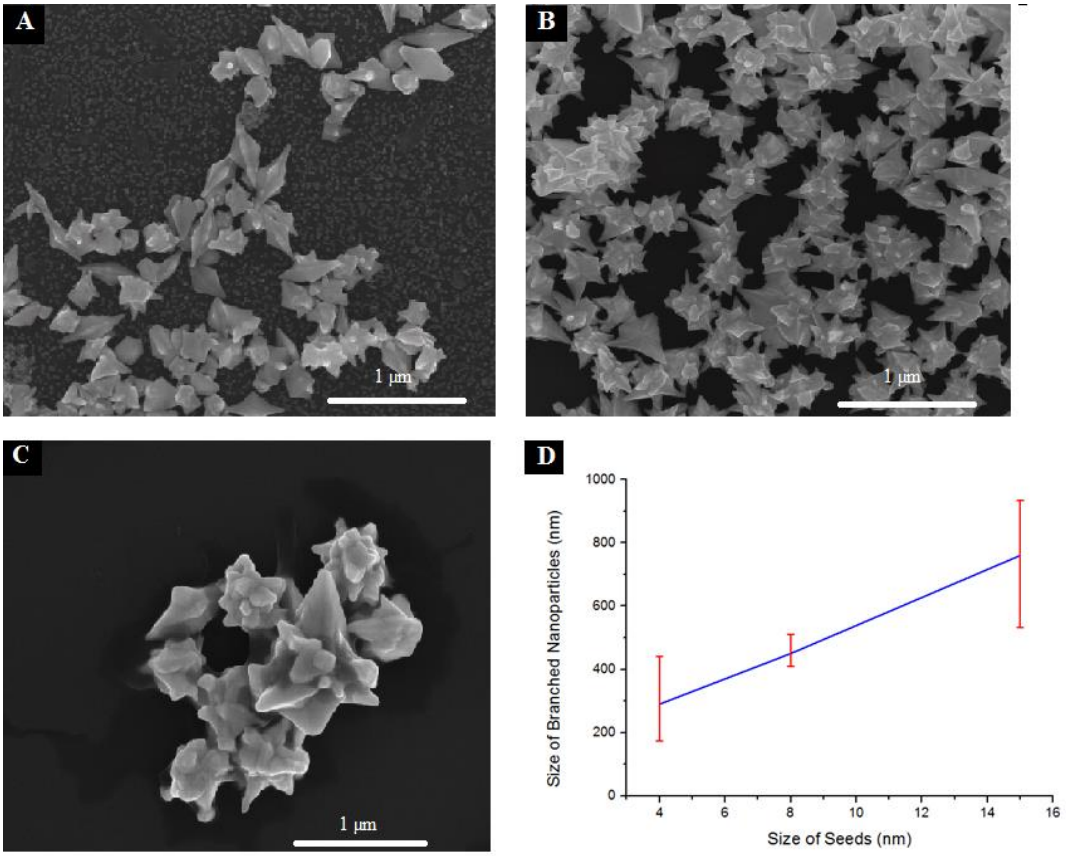

Figure 3.6. SEM images of nanoparticles grown on Si-wafer from the spherical seeds with sizes (A) 4.0 nm, (B) 8.0 nm, and (C) 15 nm as seed. Growth Solution A with a pH of ca. 3.00 was used in each set. (D) Changes in branched nanoparticle size (tip to tip distance) seed size (radius).

Besides the change in sizes of nanostructures synthesized, differences in their quality was also observed when different sizes of seeds were used. Comparison of SEM images in Figure 3.6 also shows that every seed size studied yielded some degree of branching in structures. However, yield of the ones grown from 8 nm seeds (ca. 7 particle/μm^2) are higher in terms of with respect to ones grown from 4 nm (ca. 1 particle/μm^2) and 15 nm (ca. 0.3 particle/μm^2). In addition to that while

size of the nanoparticles grown from 8 nm seeds are close to each other, the ones grown from 4 and 15 nm shows broader distribution.

3.1.2.2. Effect of Seed Morphology

Type of the seed is another parameter which may have significant impact on the morphology of the synthesized nanostructures. Recent literature is very rich on examples of using anisotropic shaped nanoparticles to synthesize new materials. For example, Kotov et al. used Au nanorods as seeds to synthesize Au nanowires.[115] Moreover, Fu et al.were able to synthesize Ag-Au bimetallic nanowires using Ag nanowires as seed. [116] Hunyadi and his co-workers also prepared Au nanotubes using Ag-Au bimetallic nanowires as seed.[117]

In this study, nanoparticles with three different morphologies (sphere, rod and star) were used as seed to investigate their effect on the structural properties of the nanoparticles grown on Si-wafer surfaces. Here, only nanostructures grown from 8 nm size spherical nanoparticles were compared with the ones obtained from rods and stars since 8 nm spherical seeds yielded the best quality nanostructures among all three sizes of spherical seeds studied. Comparison with the nanostructures synthesized from other spherical seed sizes (4 and 15 nm) are summarized in Appendices (Figure A.2 and A.3, respectively). In this part, as the seed type was changed, reactant concentrations and growth solution pH were same in each set. As it is explained in the previous part, growth solution (Growth Solution A with pH of ca.3), which was used to prepare star-shape nanoparticles was used in here.

Figure 3.7 demonstrates the SEM images of the nanostructures synthesized from three different shapes of seeds. Comparison of these results reveals that the synthesis products from spherical nanoparticle (8 nm) seeds have structural unity as well as better, more homogeneous dispersion of nanostructures on the surface. This result suggests that increased anisotropy of the seeds lead to growth of again anisotropic structures, but with decrease in the structural homogeneity. Results of using different growth media for these seeds are discussed in the following section

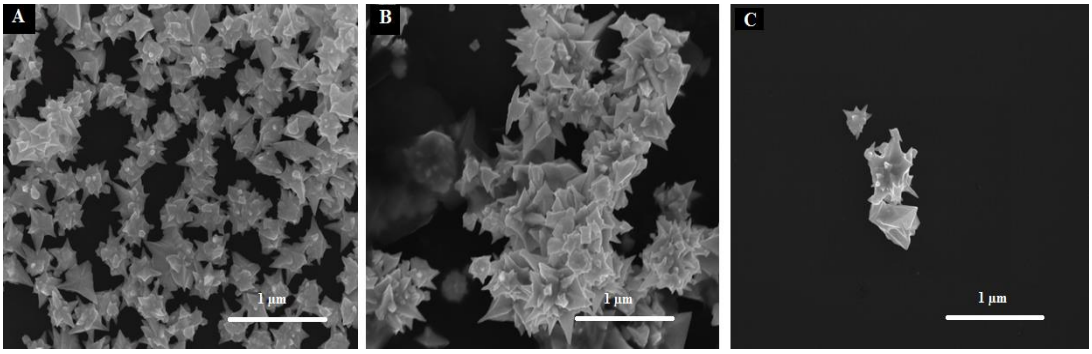

Figure 3.7. SEM images of nanoparticles grown on Si-wafer from seeds with morphologies of (A) sphere (8.0 nm) (B) rod, and (C) star. Growth solution A with a pH of ca. 3.00 was used in each set.

3.1.2.3. Effect of Growth Solution

The growth solution which contains all the reactants such as surfactant, metal salt and reducing agent play crucial role on the synthesis of nanoparticles with desired properties. The change in the type and relative concentrations of reactants can provide the manipulation of these properties.

Here, three types of growth media was studied to observe the changes in the properties of nanostructures formed. In two of the growth solutions (Growth Solution A and B) same reactants (surfactant (CTAB), metal salt ($HAuCl_4$), reducing agent (ascorbic acid) and structure directing agent ($AgNO_3$)) were used, but in different concentrations. In the third growth solution (growth solution C) except $AgNO_3$ same reactants (surfactant metal salt and reducing agent) were used as in the first two growth solutions. It should be also noted that all growth solutions investigated in this part of the study have the pH of ca.3. No attempt was made to change this value and the investigation on pH effects are discussed in the next section.

It is important to note the role of $AgNO_3$ which is still being discussed in the literature.[97,118,119] One report suggest that, in the presence of CTAB, $AgNO_3$ may cause the formation of AgBr. Ag^+ ions may adsorb onto the Au surface in the form of AgBr. That adsorption can restrict the growth.[118] More detailed explanation about the role of Ag^+ ions was given by Liu and Sionnest.[97] They proposed that a second layer of metal is formed during under potential deposition[120] process onto the preformed monolayer. This deposition process occurs at a potential less negative than the Nernst potential of the metal being deposited. As a result, Au prefers to be deposited at the (110) facets of Au, block the growth of these sites and this lead to growth from other facets.

Figure 3.8 shows the SEM images of nanostructures synthesized by using 8 nm spherical nanoparticles as seeds in three different growth solution described above. The comparison of the images suggests that the use of $AgNO_3$ in the growth solution results in the formation of branched nanoparticles. The growth solution which excludes the use of $AgNO_3$ (growth solution C) yielded nanostructures in mixed morphologies. Examining the SEM images which were taken from the different parts of the substrate shows that the first growth solution (growth solution A) lead to formation of branched nanoparticles in higher yield (ca. 7 particle/μm^2), structural

uniformity and more homogeneous dispersion on the surface compared to the ones obtained in the second growth solution (growth solution B) (ca. 5 particle/μm^2). Therefore, the first growth solution is suggested to provide better growth environment for the synthesis of branched nanostructures with desired properties.

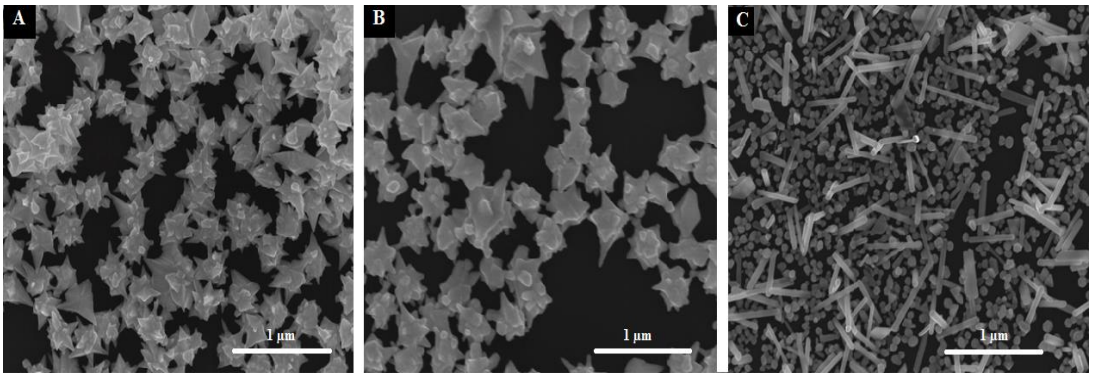

Figure 3.8. SEM images of nanoparticles grown on Si-wafer from spherical seeds (8nm) in (A) growth solution A, (B) growth solution B, and (C) growth solution C. pH of all growth solutions are ca.3.

The effect of growth solution was also studied for the seed particles with rod and star morphologies. Since the results obtained from these studies were not significant enough, they are not discussed in here. The SEM images obtained from this investigation are provided in Appendices.

3.1.2.4. Effect of pH

The pH of growth solution also affects the final shape of nanoparticles grown on Si-wafer surface. In this section, the pH of growth media is altered by adding strong acid (HCl) and base (NaOH) to the growth solution. The pH effect was investigated at four different pH values that are; strongly acidic (pH~1.45), acidic (pH~3.00), neutral (pH~7.00) and basic (pH~10.00). It should be also noted that, the results discussed here are from the sets of experiments where growth solution A and 8 nm spherical nanoparticles were used as seed.

The effect of pH change on nanoparticle morphology has been reported for various types of nanoparticles [38,44,121–123] The pH effect is better understood when the proposed ion exchange process and redox equilibrium taking place during growth of nanoparticles are considered.[38] During the growth process ion exchange between Au chloride anion ($AuCl_4^-$) and Br^- ions of CTAB to form $AuBr_4^-$ is believed to happen. Then, this ion ($AuBr_4^-$) is reduced by ascorbic acid to form Au atoms according to an equilibrium given in equation 1.

$$2\ AuBr_4^- + \text{ascorbic acid} + H_2O \Leftrightarrow 2\ Au + \text{dehydroascorbic acid} + 2\ H^+ + 4\ Br^- \quad \textbf{(3.1)}$$

According to this equilibrium, addition of acid shifts the equilibrium toward reactants and slows down the reduction process. On the other hand, base addition favor the formation of more Au atoms and promote the reaction in forward direction. Therefore, change in the pH of the growth medium has strong effect on solution dynamics and provide the possibility of controlling product properties.

Figure 3.9.B and 3.9.C shows SEM images of nanoparticles obtained in growth media with different pH values. The comparison of these images shows that the nanostructures does not have branched morphology and formed in very low yield (ca. 1 particle/μm^2) in highly acidic media (pH~1.45). The branching in the structure and the yield (ca. 7 particle/μm^2) increase significantly as the solution pH increased to ca. 3. Upon further increase in the pH value to ca. 7, nanoparticle yield is still high (ca. 7 particle/μm^2) but the branching in the morphology is lost. Finally, formation of very low numbers of nanostructures are observed as the medium become basic.

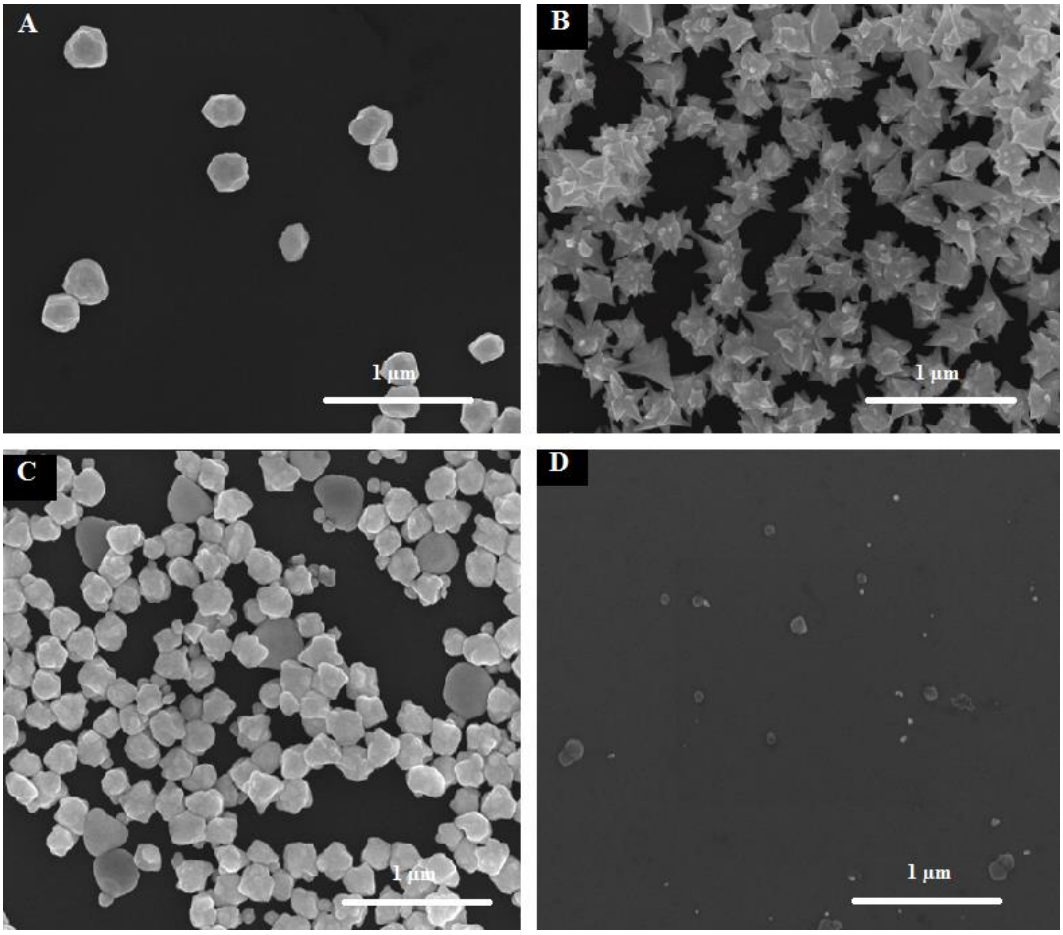

Figure 3.9. SEM images of nanoparticles growth on Si-wafer in growth solution A with and 8 nm sphere seed. (A) strongly acidic (pH~1.45) media (B) acidic (pH~3.00) media (C) neutral (pH~7.00) media (D) basic (pH~10.00) media

As it is explained above, dynamics of the growth process strongly dependent on the solution pH. Having nanostructures with no branched morphology and in very low yield at strongly acidic medium is most likely due to the suppressed reduction of Au^{3+} ions with the increase of H^{+} ions in solution. pH of 3.00 provided the optimum

medium at right acidity to form desired nanostructures. Further increase in the pH with the addition of NaOH disrupt the equilibrium toward the product side (Equation 3.1). The addition of NaOH to the growth solution to promote the reduction process and to increase anisotropesy of the nanoparticle morphology has been reported in literature.[123,124] However, in this study, NaOH addition resulted in a decrease in the anisotropy and loss of branched structure. Also, NaOH caused a change in the color of the growth solution from colorless to red which is the characteristic color of Au nanoparticles. This indicates the formation of Au nanoparticles in solution where Au^{3+} ions are readily available for the reduction. Absorption band around 520 nm in UV-Vis analysis of this solution also verify the formation of Au nanoparticles. (Figure 3.10) Zhou et al. reported that NaOH cause rapid reduction of Au ions and produce large quantity of Au atoms which grow into nanoparticles in solutions.[123] This theory agrees well with the results in this study and explains the color change in the solution.

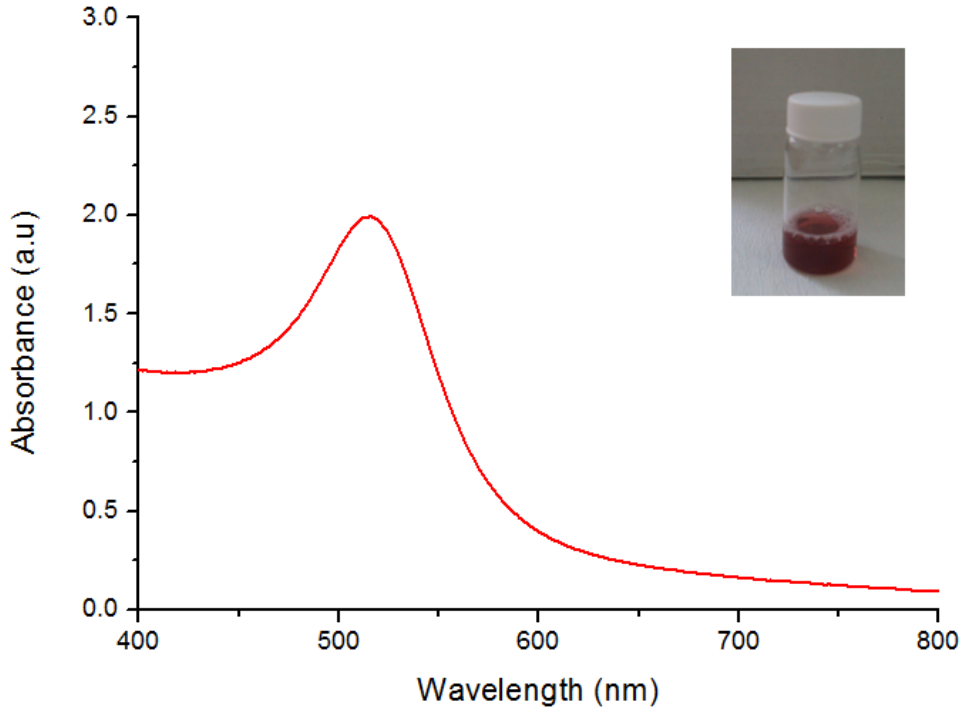

Figure 3.10. UV-Vis spectra of growth solution with NaOH. Inset shows the color of growth solution after 24 hours incubation.

Effect of pH has also been investigated for different seed types and growth solutions. Most of them did not yield nanostructures in desired morphological purity. The SEM images obtained from this investigation are given in Appendices section. (Figure A.6 and A.7). Among all the results obtained from this detailed search, it is also important to discuss the results of one particular trial where different growth solution (growth solution C) and rod nanoparticles were used as seeds. It was very exciting to see the formation of Au wires with length ca. 6.0 μm in the strongly acidic (pH~1.45) growth media. (Figure 3.11). Even though the formations of other morphologies were also observed, wires are the dominating structures in the products of growth process. The improvement of the nanowire yield requires further detailed parametric study and it is the objective of a seperate project.

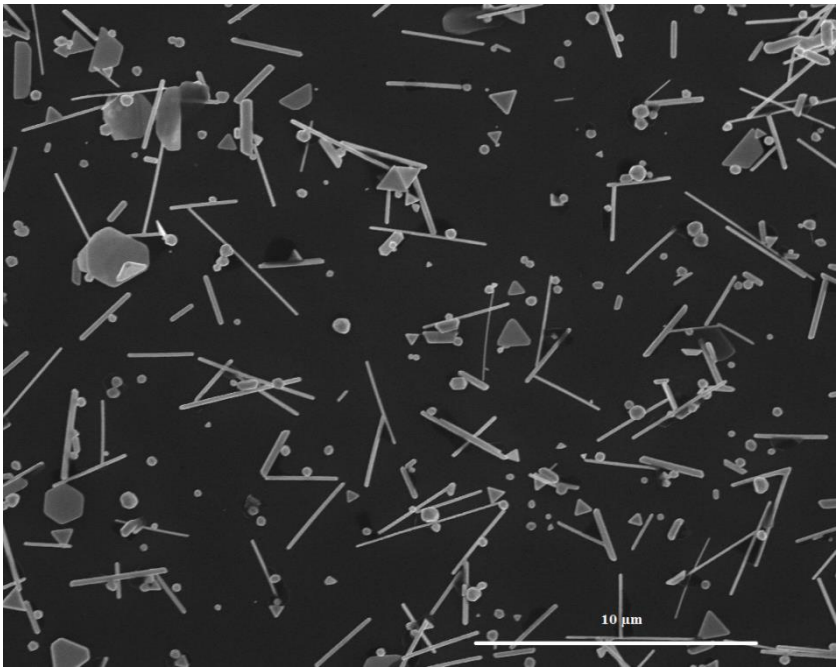

Figure 3.11. SEM images of nanoparticles growth on Si-wafer in growth solution C with 8 nm sphere seed. pH of growth solution is ca. 1.45.

3.1.3. Synthesis of Branched Gold Nanoparticles on ITO and Glass Surfaces

The parametric study revealed the best experimental condition to synthesize branched nanoparticles on Si-wafer surfaces. These conditions were also used for the synthesis of branched nanostructures on ITO and glass surfaces. The results obtained from this investigation show that same procedure can be applied to three different surfaces successfully for future potential applications of these surfaces.

Figure 3.12 and 3.13 show the SEM images of nanostructures synthesized on glass and ITO surfaces, respectively. Figure 3.14 demonstrate the comparison of nanostructures synthesized on three different surfaces. Similar to the ones on Si-wafer, these nanoparticles, too, have branched structures with various numbers of

tips were grown out of the nanoparticle core. Even though the synthesized nanoparticles have non-uniform morphologies with broad size distributions (between 350-500 nm) having all of the nanoparticles with branched morphologies suggest that high structural purity was obtained on three different surfaces. Also observing no major difference on both structures and sizes of nanoparticles synthesized on these different surfaces indicates that there is no or very insignificant effect of surface on nanoparticle morphologies. However, comparison of number of particles per unit area shows that the yield of nanoparticles on ITO surface (1.13 particle/μm^2) is significantly lower than the ones on Si-wafer (7.40 particle/μm^2) and glass surfaces (2.49 particle/μm^2). (Figure 3.15) There are two possible reasons for this observation. One of them is the loose attachment of the APTMS coated ITO surface and significant amount of nanoparticles washed out during purification process. The other reason might be the weaker interaction between APTMS and ITO surface compared to the Si-wafer and glass surfaces. As a result of this less effective binding less number of seed particles existed on the surface and finally less number of nanostructure formation occurred. Since the Au nanoparticles are expected to have strong interaction with the amine groups of APTMS and density of nanostructures formed will depend on the intensity of APTMS coverage on the surface, the first suggested reason is ruled out. Therefore, having relatively weak interaction between APTMS and ITO surface is the most likely reason for the comparably lower density of particles on this surface.

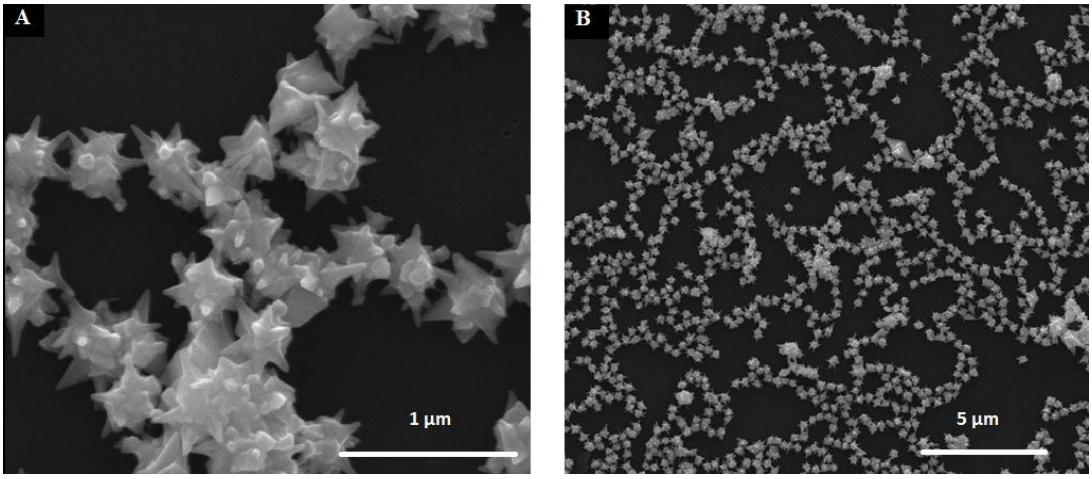

Figure 3.12. SEM images of branched Au nanoparticles synthesized on glass surfaces.

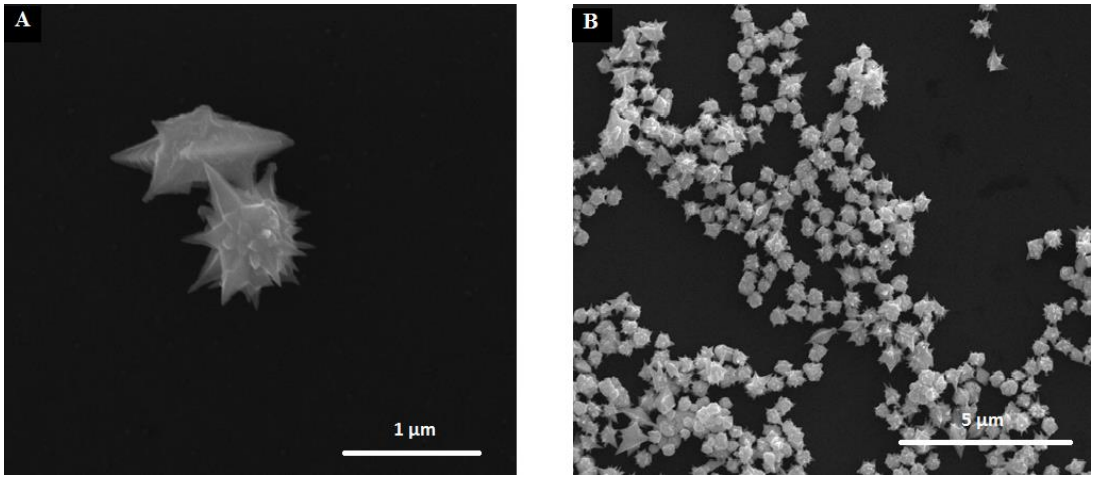

Figure 3.13. SEM images of branched Au nanoparticles synthesized on ITO surfaces.

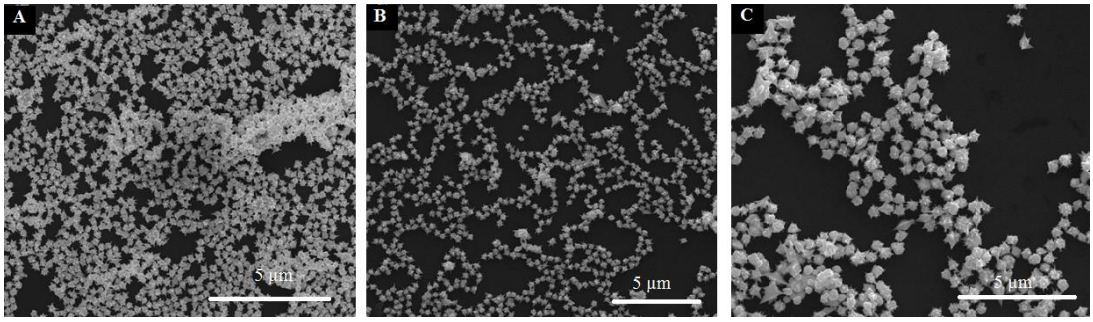

Figure 3.14. SEM images of nanoparticles grown spherical seeds (8nm), in growth solution A and on (A) Si-wafer, (B) glass, and (C) ITO surfaces. pH of all growth solutions were ca.3.00

CHAPTER 4

CONCLUSIONS

4.1. Summary of the Work

Au nanoparticles with sharp features (i.e. rod, star, branched) has become great interest due to their special optical properties which led them to be used in biosensing applications, therapeutic treatments, drug delivery and solar cell applications. Utilization of these nanoparticles in some applications requires their immobilization on surfaces. Synthesis of nanoparticles on surfaces is a practical approach to achieve this.

In this study, growth of branched Au nanoparticles on Si-wafer, glass and ITO surfaces was achieved with high structural purity and yield. Parameters such as seed type, seed size and growth media (concentration of reactants and pH of the solution) were investigated. 60 different combinations of experimental sets were tried to determine the best possible experimental conditions to synthesize nanostructures in desired properties. The results of the ones which are most meaningful were presented.

Firstly, the results from different spherical nanoparticle seed sizes (4.0, 8.0 and 15.0 nm) were compared. It was observed that as the seed size gets larger, formation of larger structures is observed. Among all seed sizes, the 8 nm ones produced branched nanoparticles in high yield (ca. 7 particle/μm^2) and morphological purity.

In the second part of the study, effect of seed nanoparticle morphology was investigated. Three different seed morphologies (sphere, rod, star) were compared. The results were shown that only spherical (8 nm) nanoparticle seeds lead to the synthesis nanostructures in desired properties with well dispersion on the surface.

In the next step of the parametric study, the reactant concentrations in the growth media were changed. Three different growth solutions, which are labelled as A, B and C, were used. The first two growth solutions contain the same reactants with different concentrations. On the other hand $AgNO_3$ which was contained in first two growth solutions (A and B), it was not added to the last one (growth solution C). The use of $AgNO_3$ made a crucial change on nanoparticle morphology and resulted in the formation of branched nanostructures.

In the last step of the parametric study, pH effect was investigated. Growth media with four different pH values were studied. These solutions were described as strongly acidic (pH~1.45), acidic (pH~3.00), neutral (pH~7.00) and basic (pH~10.00). Because of the change in the growth process dynamics upon pH change, considerable change in the nanoparticles yield and morphology was observed. The investigation showed that acidic growth media yielded the production of branched nanostrctures. In this part of the study, formation of nanowires in high yield were observed in strongly acidic solution as the growth solution (reactant concentrations) and seed type was changed.

Finally, growth of branched nanoparticles on ITO and Si-wafer surfaces were achieved. The optimum experimental conditions which were derived from the parametric study was used. The use of different substrates did not make significant change on nanoparticle properties. However, the nanostructure yield on ITO was observed to be lower compared to other surfaces.

As a result, facile way of synthesizing branched Au nanoparticles were demonstrated in this study. Having special optical properties inherited by nanostructures synthesized on different surfaces makes the fabricated systems very promising for various nanotechnology applications.

4.2. Future Work

In this thesis, Au nanoparticles with branched morphologies were achieved on three different substrate surfaces; Si wafer, glass and ITO by investigating parameters such as seed type, seed size and growth media. During the investigation of parameters, the synthesis of Au wires with length ca. 6.0 μm were also achieved under different conditions than the ones of branched nanoparticles. Even though the presences of nanoparticles with other morphologies were also observed, wires were dominating morphology among the products of this synthesis. Nanowires with high aspect ratios are very interesting since they have potential uses in nanocircuit fabrication for conductivity and optical measurements and plasmonic antenna fabrication. Obtaining long nanowires with high structural purity and yield would require further detailed parametric study. This could be achieved by modifying concentration of reactants and/or use of acids which will make growth process slower. Moreover, after purification of substrates from the undesirable morphologies, substrates may be exposed to a second growth solution for further growth of nanowires.

In addition, possible applications of branched gold nanoparticles as well as nanowires grown on surfaces will be a subject for future work. Implementation of these nanoparticles in solar cells, light emitting diodes and SERS will be investigated.

REFERENCES

(1) Nalbant Esenturk, E.; Hight Walker, A. R. *J. Raman Spectrosc.* **2009**, *40*, 86–91.

(2) Jeong, G. H.; Lee, Y. W.; Kim, M.; Han, S. W. *J. Colloid Interface Sci.* **2009**, *329*, 97–102.

(3) Yi, S.; Sun, L.; Lenaghan, S. C.; Wang, Y.; Chong, X.; Zhang, Z.; Zhang, M. *RSC Adv.* **2013**, *3*, 10139.

(4) Kozanoglu, D.; Apaydin, D. H.; Cirpan, A.; Esenturk, E. N. *Org. Electron.* **2013**, *14*, 1720–1727.

(5) Li, N.; Zhao, P.; Astruc, D. *Angew. Chem. Int. Ed. Engl.* **2014**, *53*, 1756–1789.

(6) Viswanathan, B. *Nano Materials*; Alpha Acience International Ltd.: Oxford, **2009**; pp. 35–52.

(7) Jin, Y.; Li, Q.; Li, G.; Chen, M.; Liu, J.; Zou, Y.; Jiang, K.; Fan, S. *Nanoscale Res. Lett.* **2014**, *9*, 7.

(8) Huang, X.; El-Sayed, I. H.; Qian, W.; El-Sayed, M. a. *J. Am. Chem. Soc.* **2006**, *128*, 2115–2120.

(9) Nalbant Esenturk, E. *J. Raman Spectrosc.* **2009**, *40*, 86–91.

(10) Johnson, C.; Dujardin, E. *J. Mater. Chem.* **2002**, *12*, 1765–1770.

(11) Huang, X.; Neretina, S.; El-Sayed, M. *Adv. Mater.* **2009**, *21*, 4880–4910.

(12) Murphy, C. J.; Sau, T. K.; Gole, A. M.; Orendorff, C. J.; Gao, J.; Gou, L.; Hunyadi, S. E.; Li, T. *J. Phys. Chem. B* **2005**, *109*, 13857–13870.

(13) Liu, J.; He, F.; Gunn, T. M.; Zhao, D.; Roberts, C. B. *Langmuir* **2009**, *25*, 7116–7128.

(14) Taub, N.; Krichevski, O.; Markovich, G. *J. Phys. Chem. B* **2003**, *107*, 11579–11582.

(15) Kambayashi, M.; Zhang, J.; Oyama, M. *Cryst. Growth Des.* **2005**, *5*, 81–84.

(16) Bhushan, B. *Springer Handbook of Nanotechnology*; **2010**; pp. 1–14.

(17) Colomban, P. and G. G. *Ann. Chim.* **2005**, *30*, 1–16.

(18) Sánchez del Río, M.; Martinetto, P.; Reyes-Valerio, C.; Dooryhée, E.; Suárez, M. *Archaeometry* **2006**, *48*, 115–130.

(19) Leonhardt, U. *Nat. Photonics* **2007**, *1*, 207–208.

(20) Dekkers, S.; Krystek, P.; Peters, R. J. B.; Lankveld, D. P. K.; Bokkers, B. G. H.; van Hoeven-Arentzen, P. H.; Bouwmeester, H.; Oomen, A. G. *Nanotoxicology* **2011**, *5*, 393–405.

(21) Nohynek, G. J.; Lademann, J.; Ribaud, C.; Roberts, M. S. *Crit. Rev. Toxicol.* **2007**, *37*, 251–277.

(22) Faraday, M. *Philos. Transations R. Soc. London.* **1857**, *147*, 145–181.

(23) Sweeney, A. *Sci. Eng. Ethics* **2006**, *12*, 435–464.

(24) Lu, K. *Nanoparticle Materials: Synthesis, Characterization and Processing*; John Wiley & Sons: New Jersey, **2013**; pp. 1–20.

(25) Sajanlal, P. R.; Sreeprasad, T. S.; Samal, A. K.; Pradeep, T. *Nano Rev.* **2011**, *2*, 5883–5945.

(26) Paulus, P.; Goossens, A.; Thiel, R.; van der Kraan, A.; Schmid, G.; de Jongh, L. *Phys. Rev. B* **2001**, *64*, 205418–205436.

(27) Sarkar, M.; Datta, J.; Mondal, D.; Mukhopadhyay, S. *Int. J. Res. Eng. Technol.* **2013**, *02*, 400–404.

(28) Zhang, Z.; Sun, X.; Dresselhaus, M.; Ying, J.; Heremans, J. *Phys. Rev. B* **2000**, *61*, 4850–4861.

(29) Chung, S.-W.; Yu, J.-Y.; Heath, J. R. *Appl. Phys. Lett.* **2000**, *76*, 2068.

(30) Eustis, S.; el-Sayed, M. a. *Chem. Soc. Rev.* **2006**, *35*, 209–217.

(31) Siekkinen, A.; Xia, Y. *J. Phys. Chem. Soc* **2006**, *110*, 15666–15675.

(32) Schmid, G. *Nanoparticles: From Theory to Application*; Wiley-VCH: Weinheim, **2004**; pp. 4–42.

(33) Issa, B.; Obaidat, I.; Albiss, B. ; Haik, Y. *Int. J. Mol. Sci.* **2013**, *14*, 21266–21305.

(34) Moskovits, M. *J. Chem. Phys.* **1978**, *69*, 4159.

(35) Keating, C. D.; Kovaleski, K. K.; Natan, M. J. *J. Phys. Chem. B* **1998**, *102*, 9414–9425.

(36) Search, H.; Journals, C.; Contact, A.; Iopscience, M.; Electron, Q.; Address, I. P. *Quantum Electron* **1993**, *23*, 435–440.

(37) Teo, B. K.; Sun, X. H. *J. Clust. Sci.* **2007**, *18*, 346–357.

(38) Wang, Y. N.; Wei, W. T.; Yang, C. W.; Huang, M. H. *Langmuir* **2013**, *29*, 10491–10497.

(39) Murphy, C. J.; Jana, N. R. *Adv. Mater.* **2002**, *14*, 80–82.

(40) Sau, T. K.; Murphy, C. J. *Langmuir* **2004**, *20*, 6414–6420.

(41) Perezjuste, J.; Pastorizasantos, I.; Lizmarzan, L.; Mulvaney, P. *Coord. Chem. Rev.* **2005**, *249*, 1870–1901.

(42) Jiang, X. C.; Brioude, a.; Pileni, M. P. *Colloids Surfaces A Physicochem. Eng. Asp.* **2006**, *277*, 201–206.

(43) Jiang, X. C.; Pileni, M. P. *Colloids Surfaces A Physicochem. Eng. Asp.* **2007**, *295*, 228–232.

(44) Kim, F.; Sohn, K.; Wu, J.; Huang, J. *J. Am. Chem. Soc.* **2008**, *130*, 14442–14443.

(45) Xu, C. L.; Zhang, L.; Zhang, H. L.; Li, H. L. *Appl. Surf. Sci.* **2005**, *252*, 1182–1186.

(46) Hu, J.; Odom, T. W.; Lieber, C. M. *Acc. Chem. Res.* **1999**, *32*, 435–445.

(47) Chu, H.; Kuo, C.; Huang, M. *Inorg. Chem.* **2006**, *45*, 808–813.

(48) Sajanlal, P. R.; Subramaniam, C.; Sasanpour, P.; Rashidian, B.; Pradeep, T. *J. Mater. Chem.* **2010**, *20*, 2108.

(49) Sun, X.; Dong, S.; Wang, E. *Langmuir* **2005**, *21*, 4710–4712.

(50) Ah, C.; Yun, Y.; Park, H.; Kim, W. *Chem. Mater.* **2005**, *17*, 5558–5561.

(51) Sun, C.; Linn, N.; Jiang, P. *Chem. Mater.* **2007**, 4551–4556.

(52) Li, G.; Li, H.; Ho, J. Y. L.; Wong, M.; Kwok, H. S. *Nano Lett.* **2014**, *14*, 2563–2568.

(53) Khoury, C. G.; Vo-Dinh, T. *J. Phys. Chem. C* **2008**, *112*, 18849–18859.

(54) Kumar, P. S.; Santos, I. P.; Gonzalez, B. R.; Abajo, J. G.; Marzan, L. L. *Nanotechnology* **2008**, *19*, 1–7.

(55) Ge, J.; Lei, J.; Zare, R. N. *Nat. Nanotechnol.* **2012**, *7*, 428–432.

(56) Chen, J.; Yang, M.; Zhang, Q.; Cho, E. C.; Cobley, C. M.; Kim, C.; Glaus, C.; Wang, L. V.; Welch, M. J.; Xia, Y. *Adv. Funct. Mater.* **2010**, *20*, 3684–3694.

(57) Liao, H.; Hafner, J. *Chem. Mater.* **2005**, *5*, 4636–4641.

(58) Chen, J.; Saeki, F.; Wiley, B. J.; Cang, H.; Cobb, M. J.; Li, Z.-Y.; Au, L.; Zhang, H.; Kimmey, M. B.; Li, X.; Xia, Y. *Nano Lett.* **2005**, *5*, 473–477.

(59) Gu, C.; Zhang, T. *Langmuir* **2008**, 12010–12016.

(60) Aslan, K.; Lakowicz, J. R.; Geddes, C. D. *Curr. Opin. Chem. Biol.* **2005**, *9*, 538–544.

(61) Gimeno, C. In *Modern Supramolecular Gold Chemistry: Gold Metal Interactions and Applications*; **2009**; pp. 1–64.

(62) Bi, N.; Chen, Y.; Qi, H.; Zheng, X.; Chen, Y.; Liao, X.; Zhang, H.; Tian, Y. *Sensors Actuators B Chem.* **2012**, *166-167*, 766–771.

(63) Bi, H.; Lapierre, R. R. *Nanotechnology* **2009**, *20*, 465205.

(64) Zhou, Y.; Eck, M.; Krüger, M. *Energy Environ. Sci.* **2010**, *3*, 1851.

(65) Moulé, A. J.; Bonekamp, J. B.; Meerholz, K. *J. Appl. Phys.* **2006**, *100*, 1–8.

(66) Mahmoud, A. Y.; Zhang, J.; Ma, D.; Izquierdo, R.; Truong, V.-V. *Org. Electron.* **2012**, *13*, 3102–3107.

(67) Peet, J.; Wen, L.; Byrne, P.; Rodman, S.; Forberich, K.; Shao, Y.; Drolet, N.; Gaudiana, R.; Dennler, G.; Waller, D. *Appl. Phys. Lett.* **2011**, *98*, 043301.

(68) Fung, D. D. S.; Qiao, L.; Choy, W. C. H.; Wang, C.; Sha, W. E. I.; Xie, F.; He, S. *J. Mater. Chem.* **2011**, *21*, 16349.

(69) Wang, C. C. D.; Choy, W. C. H.; Duan, C.; Fung, D. D. S.; Sha, W. E. I.; Xie, F.-X.; Huang, F.; Cao, Y. *J. Mater. Chem.* **2012**, *22*, 1206.

(70) Kim, I.; Lee, T. S.; Jeong, D. S.; Lee, W. S.; Lee, K.-S. *J. Phys. D. Appl. Phys.* **2012**, *45*, 1–6.

(71) Stavytska-Barba, M.; Salvador, M.; Kulkarni, A.; Ginger, D. S.; Kelley, A. M. *J. Phys. Chem. C* **2011**, *115*, 20788–20794.

(72) Maier, S.; Kik, P. *Mater. Res. Soc.* **2003**, *777*, 1–12.

(73) Maier, S.; Kik, P.; Atwater, H.; Meltzer, S. *Nat. Mater.* **2003**, *2*, 229–232.

(74) Cho, C.-Y.; Kim, K. S.; Lee, S.-J.; Kwon, M.-K.; Ko, H.; Kim, S.-T.; Jung, G.-Y.; Park, S.-J. *Appl. Phys. Lett.* **2011**, *99*, 041107.

(75) Behari, J. *Indian J. Exp. Biol.* **2010**, *48*, 1008–1019.

(76) Reetz, M. T.; Helbig, W. *J. Am. Chem. Soc.* **1994**, *116*, 7401–7402.

(77) Huang, C.-J.; Wang, Y.-H.; Chiu, P.-H.; Shih, M.-C.; Meen, T.-H. *Mater. Lett.* **2006**, *60*, 1896–1900.

(78) Porter, L.; Choi, H.; Ribbe, A.; Buriak, J. *Nano Lett.* **2002**, *2*, 1067–1071.

(79) Kim, F.; Song, J.; Yang, P. *J. Am. Chem. Soc.* **2002**, *124*, 14316–14317.

(80) Ahmed, M.; Narain, R. *Langmuir* **2010**, *26*, 18392–18399.

(81) Mcgilvray, K. L.; Decan, M. R.; Wang, D.; Scaiano, J. C. *J. Am. Chem. Soc.* **2006**, *128*, 15980–15981.

(82) Fievet, F.; Lagier, J.; Figlarz, M. *MRS Bull* **1989**, 29–34.

(83) Viau, G.; Fihet, F. *Solid State Ionics* **1996**, *84*, 259–270.

(84) Hayashi, H.; Hakuta, Y. *Materials (Basel).* **2010**, *3*, 3794–3817.

(85) Lu, C.; Qi, L.; Yang, J.; Tang, L.; Zhang, D.; Ma, J. *Chem. Commun. (Camb).* **2006**, 3551–3553.

(86) Dertli, E.; Coskun, S.; Esenturk, E. N. *J. Mater. Res.* **2013**, *28*, 250–260.

(87) Jana, N. R.; Gearheart, L.; Murphy, C. J. *Adv. Mater.* **2001**, *13*, 1389–1393.

(88) Mallick, K.; Wang, Z. L.; Pal, T. *J. Photochem. Photobiol. A Chem.* **2001**, *140*, 75–80.

(89) Niu, W.; Zhang, L.; Xu, G. *Nanoscale* **2013**, *5*, 3172–3181.

(90) Turkevich, J.; Stevenson, P. C.; Hillier, J. *Discuss Faraday* **1951**, *11*, 55–75.

(91) Goia, D. *New J. Chem.* **1998**, 1203–1215.

(92) Jana, N.; Gearheart, L.; Murphy, C. *Chem. Mater.* **2001**, 2313–2322.

(93) Jana, N. R.; Gearheart, L.; Murphy, C. J. *J. Phys. Chem. B* **2001**, *105*, 4065–4067.

(94) Nikoobakht, B.; El-Sayed, M. *Chem. Mater.* **2003**, 1957–1962.

(95) Nikoobakht, B.; Wang, Z. L.; El-Sayed, M. a. *J. Phys. Chem. B* **2000**, *104*, 8635–8640.

(96) Gole, A.; Murphy, C. J. *Chem. Mater.* **2004**, *16*, 3633–3640.

(97) Liu, M.; Guyot-sionnest, P. *J. Phys. Chem. B* **2005**, *109*, 22192–22200.

(98) Rojas, M.; Sanchez, C. *Surf. Sci.* **2000**, *453*, 225–228.

(99) Orendorff, C. J.; Murphy, C. J. *J. Phys. Chem. B* **2006**, *110*, 3990–3994.

(100) Burda, C.; Chen, X.; Narayanan, R.; El-Sayed, M. a. *Chem. Rev.* **2005**, *105*, 1025–1102.

(101) Boca, S.; Rugina, D.; Pintea, A.; Barbu-Tudoran, L.; Astilean, S. *Nanotechnology* **2011**, *22*, 1–7.

(102) Jena, B.; Raj, C. *Langmuir* **2007**, 15707–15713.

(103) Bakr, O.; Wunsch, B.; Stellacci, F. *Chem. Mater.* **2006**, *18*, 3297–3301.

(104) Darwich, S. Colloidal Gold Nanoparticules : A study of their Drying-Mediated Assembly in Mesoscale Aggregation Patterns and of their AFM Assisted Nanomanipulation on Model Solid Surfaces, Haute-Alsace, **2011**.

(105) Nehl, C. L.; Liao, H.; Hafner, J. H. *Nano Lett.* **2006**, *6*, 683–688.

(106) Shipway, A. N.; Katz, E.; Willner, I. *ChemPhysChem* **2000**, *1*, 18–52.

(107) Chaikin, Y.; Kedem, O.; Raz, J.; Vaskevich, A.; Rubinstein, I. *Anal. Chem.* **2013**, *85*, 10022–10027.

(108) Kinge, S.; Crego-Calama, M.; Reinhoudt, D. N. *ChemPhysChem* **2008**, *9*, 20–42.

(109) Harnisch, J. A.; Pris, A. D.; Porter, M. D.; March, R. V. *J. Am. Chem. Soc* **2001**, *123*, 5829–5830.

(110) Chumanov, G.; Sokolov, K.; Gregory, B. W.; Cotton, T. M. *J. Phys. Chem.* **1995**, *99*, 9466–9471.

(111) Cheng, W.; Dong, S.; Wang, E. *Anal. Chem.* **2002**, *74*, 3599–3604.

(112) Grabar, K. C.; Freeman, R. G.; Hommer, M. B.; Natan, M. J. *Anal. Chem.* **1995**, *67*, 1217–1225.

(113) Li, C.; Su, Y.; Lv, X.; Xia, H.; Wang, Y. *Sensors Actuators B Chem.* **2010**, *149*, 427–431.

(114) Talapin, D. V.; Rogach, A. L.; Haase, M.; Weller, H. *J. Phys. Chem. B* **2001**, *105*, 12278–12285.

(115) Critchley, K.; Khanal, B. P.; Górzny, M. Ł.; Vigderman, L.; Evans, S. D.; Zubarev, E. R.; Kotov, N. a. *Adv. Mater.* **2010**, *22*, 2338–2342.

(116) Fu, H.; Yang, X.; Jiang, X.; Yu, A. *Langmuir* **2013**, *29*, 7134–7142.

(117) Hunyadi, S. E.; Murphy, C. J. *J. Mater. Chem.* **2006**, *16*, 3929.

(118) Grzelczak, M.; Pérez-Juste, J.; Mulvaney, P.; Liz-Marzán, L. M. *Chem. Soc. Rev.* **2008**, *37*, 1783–1791.

(119) Sudha, V.; Sangaranarayanan, M. V. *J. Phys. Chem. B* **2002**, *106*, 2699–2707.

(120) Rogers, L. B.; Ridge, O. *J. Electrochem. Soc.* **1948**, *95*, 33–46.

(121) Sau, T.; Murphy, C. *J. Am. Chem. Soc.* **2004**, 8648–8649.

(122) Zhu, C.; Peng, H.-C.; Zeng, J.; Liu, J.; Gu, Z.; Xia, Y. *J. Am. Chem. Soc.* **2012**, *134*, 20234–20237.

(123) Zhou, J.; Zeng, J.; Grant, J.; Wu, H.; Xia, Y. *Small* **2011**, *7*, 3308–3316.

(124) Guerrero-Martínez, A.; Barbosa, S.; Pastoriza-Santos, I.; Liz-Marzán, L. M. *Curr. Opin. Colloid Interface Sci.* **2011**, *16*, 118–127.

(125) Waterland, M. Nanoscience http://nanoscience.massey.ac.nz/ (accessed Dec 8, 2014).

(126) The British Museum Trustees http://www.britishmuseum.org/about_us/management/trustees.aspx (accessed Dec 23, 2014).

(127) Tweney, R. Faraday's Gold http://aveburybooks.com/faraday/catalog.html (accessed Nov 13, 2014).

(128) Chukwuocha, E. O.; Onyeaju, M. C.; Harry, T. S. T. *World J. Condens. Matter Phys.* **2012**, *2*, 96–100.

(129) Dreaden, E. C.; Alkilany, A. M.; Huang, X.; Murphy, C. J.; El-Sayed, M. a. *Chem. Soc. Rev.* **2012**, *41*, 2740–2779.

(130) Smith, D.; Korgel, B. *Langmuir* **2008**, 644–649.

APPENDIX A

FIGURES RELATIVE TO CHAPTER 3

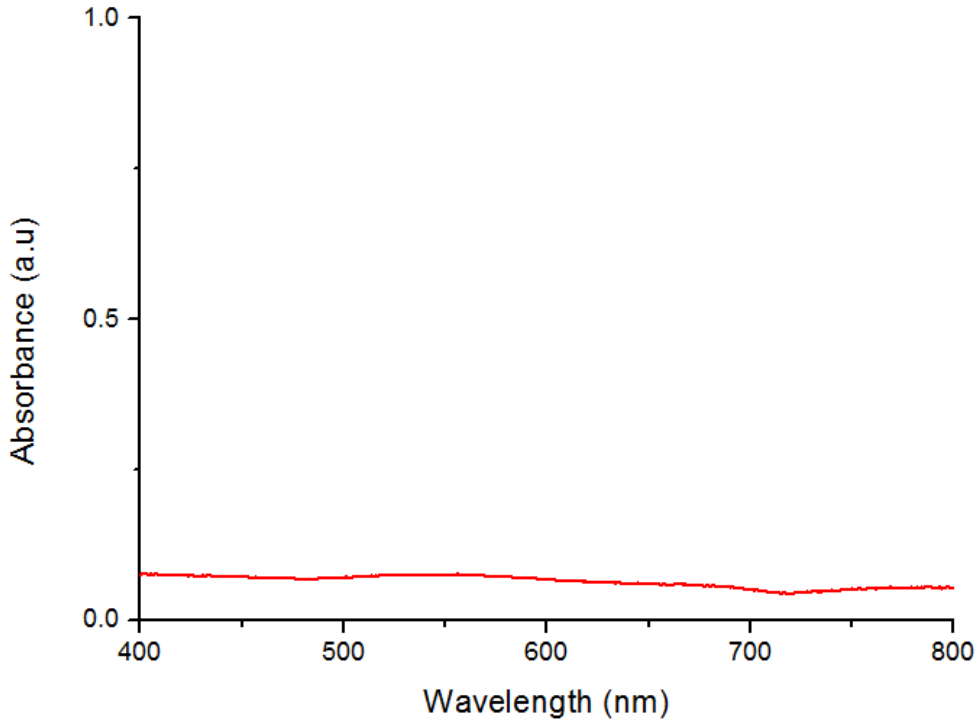

Figure A.1. UV-Vis Spectra of Growth Solution after 24 hour incubation of substrate.

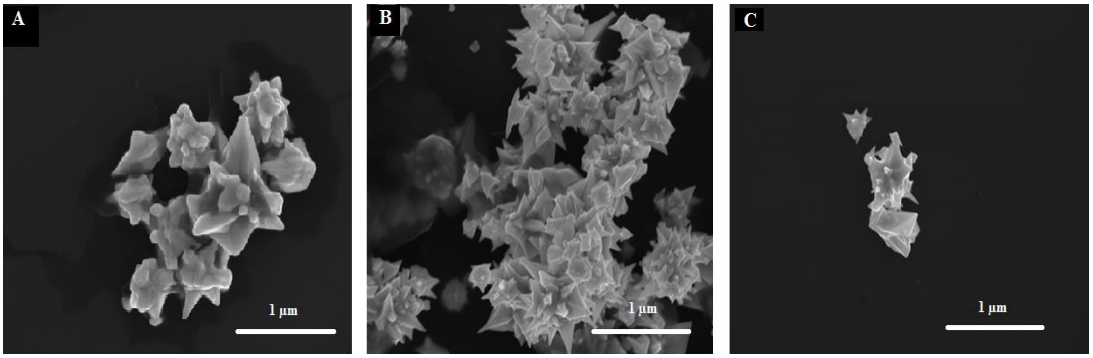

Figure A.3. SEM images of nanoparticles grown on Si-wafer from seeds with morphologies of (A) sphere (15.0 nm) (B) rod, and (C) star. Growth solution A with a pH of ca. 3.00 was used in each set.

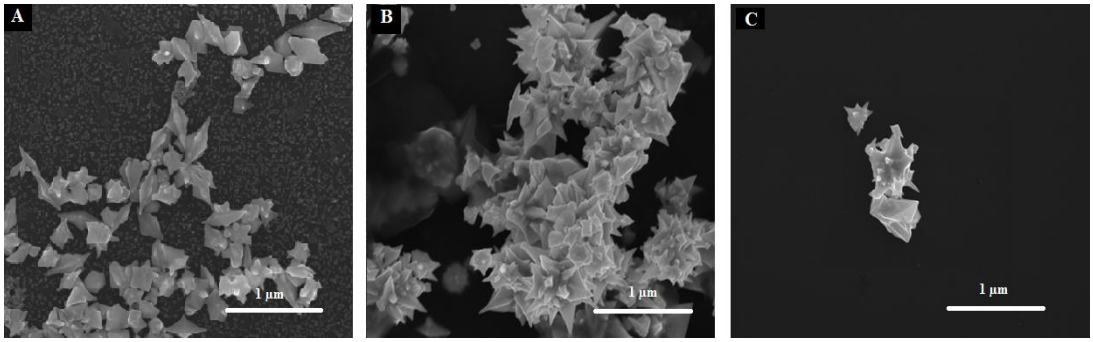

Figure A.2 SEM images of nanoparticles grown on Si-wafer from seeds with morphologies of (A) sphere (4.0 nm) (B) rod, and (C) star. Growth solution A with a pH of ca. 3.00 was used in each set.

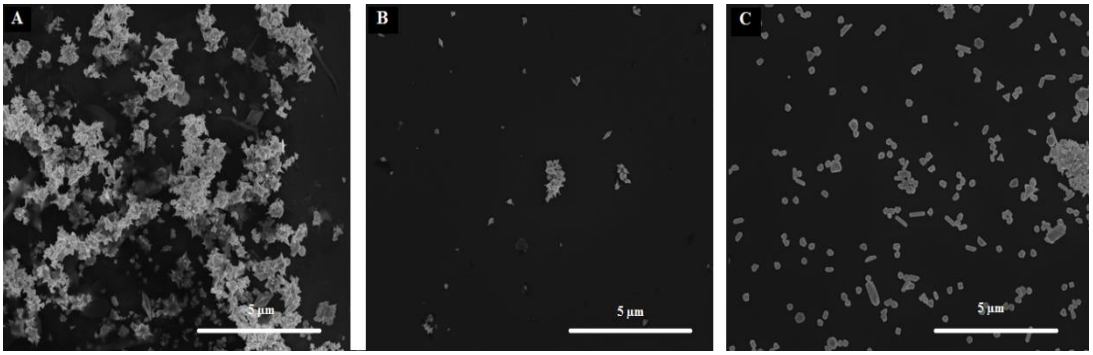

Figure A.4. SEM images of nanoparticles grown on Si-wafer from rod shaped seed in (A) growth solution A, (B) growth solution B, and (C) growth solution C. pH of all growth solutions are ca.3.00

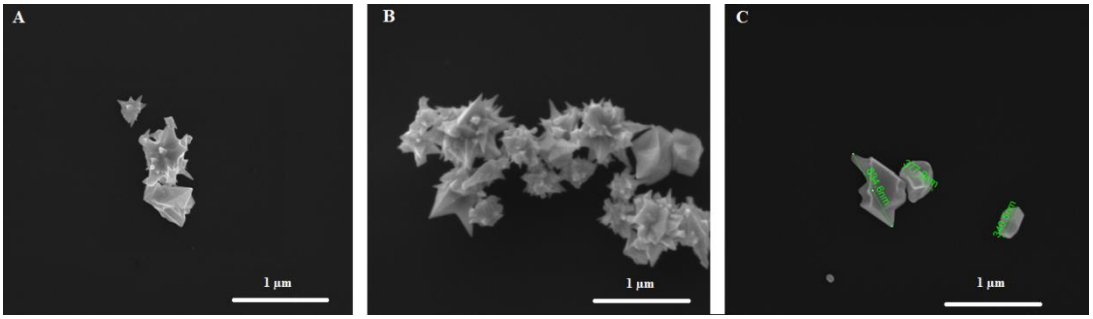

Figure A.5. SEM images of nanoparticles grown on Si-wafer from star shaped seed in (A) growth solution A, (B) growth solution B, and (C) growth solution C. pH of all growth solutions are ca.3.00

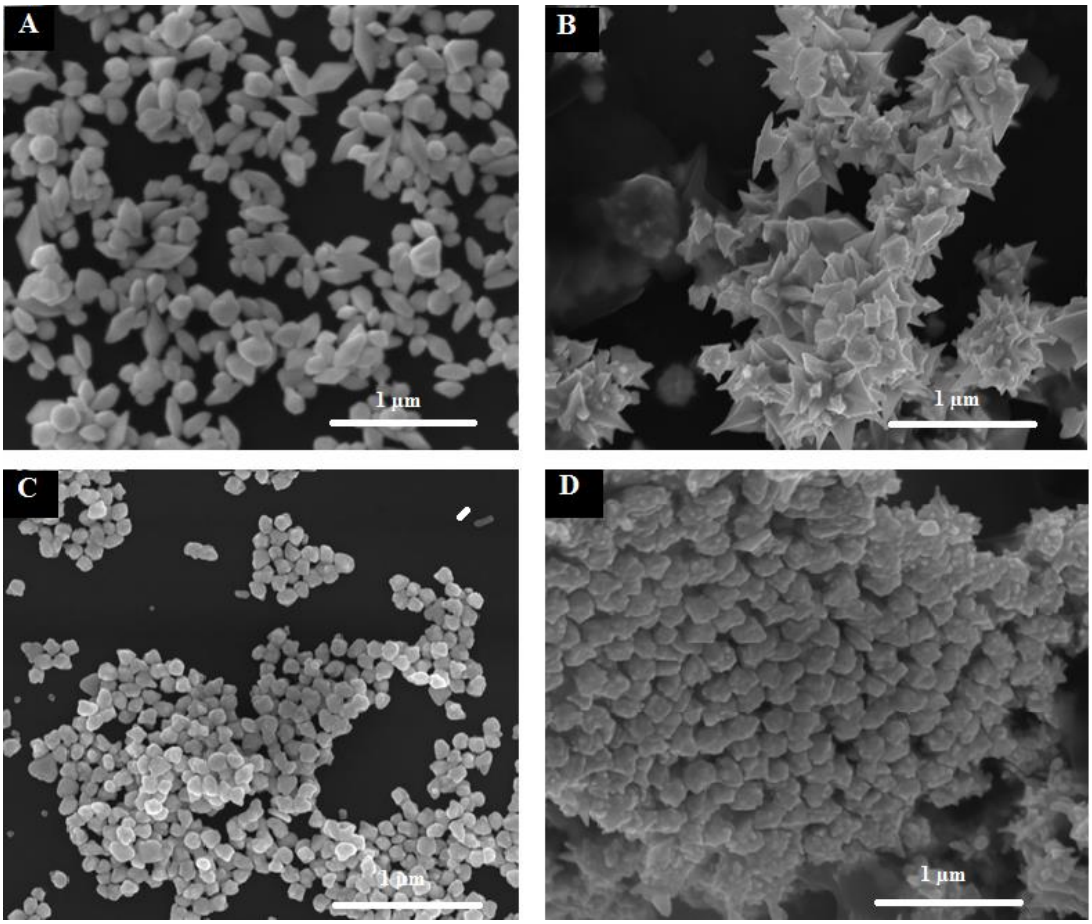

Figure A.6. SEM images of nanoparticles grown from rod shaped seed, on Si-wafer and in Growth Solution A. (A) Strongly Acidic (pH~1.45) Media (B) Acidic (pH~3.00) Media (C) Neutral (pH~7.00) Media (D) Basic (pH~10.00) Media

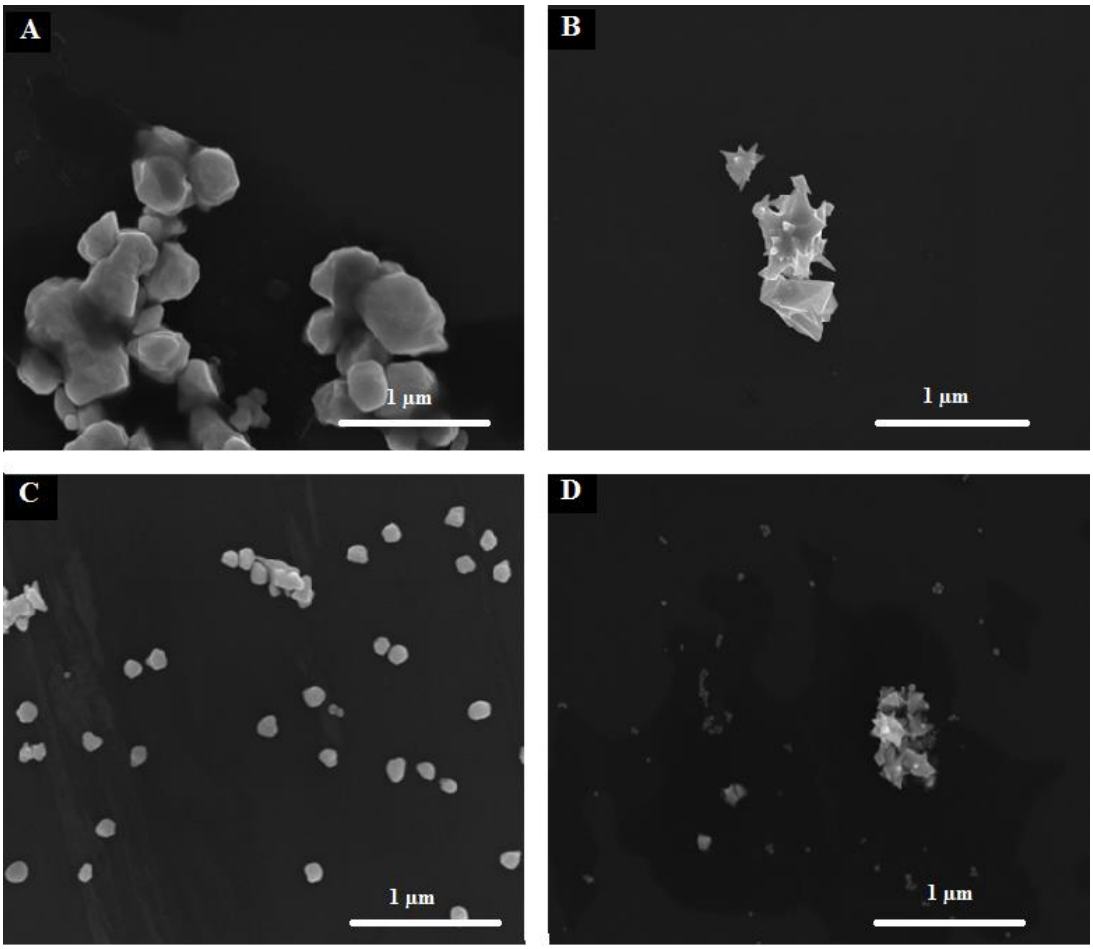

Figure A.7. SEM images of nanoparticles grown from star shaped seed, on Si-wafer and in Growth Solution A. (A) Strongly Acidic (pH~1.45) Media (B) Acidic (pH~3.00) Media (C) Neutral (pH~7.00) Media (D) Basic (pH~10.00)

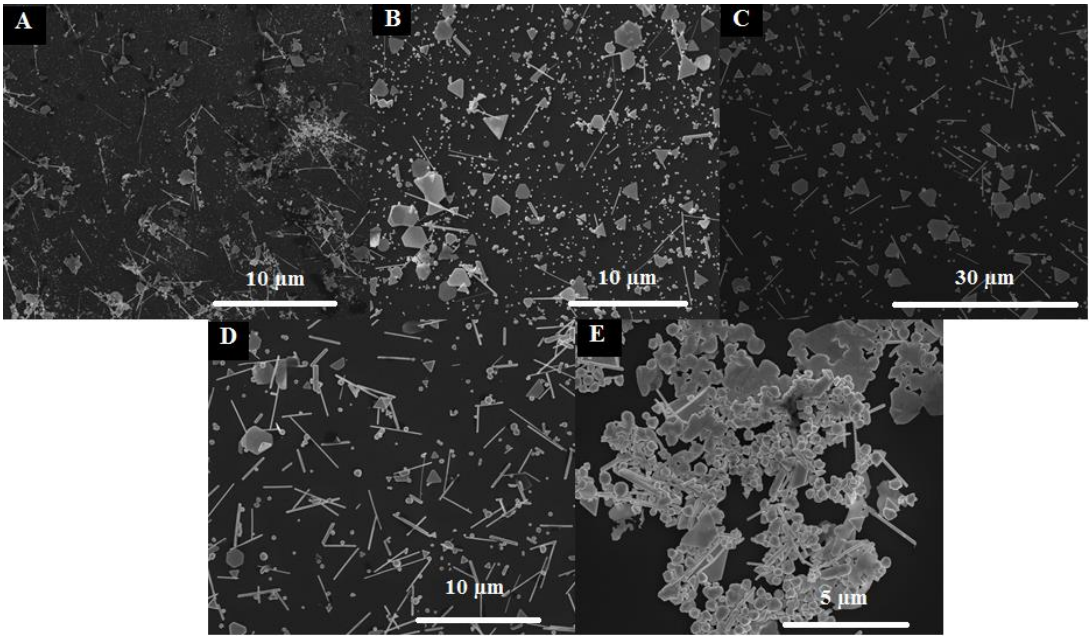

Figure A.8. SEM images of nanoparticles grown on Si-wafer from seeds (A) 4.0 nm, (B) 8.0 nm, and (C) 15 nm (D) rod and (E) star as seed. Growth Solution C with a pH of ca. 1.45 was used in each set.